TSC2 acting as a transcription factor for miR-514b-3p and regulating PI3K-AKT-MTOR pathway via nucleus

Sakshi Gupta*#, Naresh Mahajan*, Mukund Kumar*, and Arun Kumar*#

*Department of Developmental Biology and Genetics, Indian Institute of Science, Bangalore, 560012

#Joint corresponding authors:

Email ID: sakshigupta1@iisc.ac.in

Email ID: arunk@iisc.ac.in

ORCID IDs:

Sakshi Gupta: 0000-0001-5820-2391

Arun Kumar: 0000-0003-0537-6560

Keywords: TSC2, miR-514b-3p, TSPAN9, transcription factor, gene regulation, PI3K-AKT-MTOR

Abstract

The PI3K-AKT-MTOR signalling axis is pivotal in regulating cell survival, proliferation, and growth. TSC2 (tuberous sclerosis complex subunit 2) is a well-established negative regulator of this pathway, which primarily acts by suppressing the MTORC1 activity. While the cytoplasmic role of TSC2 is well characterized, emerging evidence suggests its additional nuclear functions. Previous work from our laboratory identified TSC2 as a transcriptional repressor of the *EREG* (Epiregulin) gene. Building on this foundation, the present study investigates the transcriptional role of TSC2 in miRNA (microRNA) gene regulation. A genome-wide miRNA microarray profiling of TSC2-depleted cells from an oral squamous cell carcinoma (OSCC) cell line, SCC131, identified 19 upregulated and 24 downregulated miRNAs. Of them, miR-514b-3p emerged as one of the most significantly upregulated miRNAs. TSC2 knockdown resulted in robust miR-514b-3p upregulation, whereas TSC2 overexpression suppressed its expression. Moreover, TSC2 negatively regulates *MIR514B* promoter activity in an NLS-dependent manner. The chromatin immunoprecipitation analysis showed direct binding between TSC2 and *MIR514B* promoter, establishing miR-514b-3p as a transcriptional target of TSC2. We further identified *TSPAN9* (Tetraspanin 9) as a direct downstream target of miR-514b-3p. The dual-luciferase reporter assay and Western blot analysis confirmed direct interaction between miR-514b-3p and *TSPAN9* 3'UTR. Furthermore, TSC2 positively regulates *TSPAN9* levels by repressing miR-514b-3p, thereby establishing a novel TSC2-miR-514b-3p-TSPAN9 regulatory axis. Additionally, we uncovered crosstalk between TSC2-miR-514b-3p-TSPAN9 axis and the canonical PI3K-AKT-MTOR signalling, where miR-514b-3p positively, and *TSPAN9* negatively regulates the PI3K-AKT-MTOR pathway. Interestingly, AKT functions as an upstream regulator of this axis by modulating TSC2 nuclear localization. Collectively, this study provides new insights into the non-canonical, nucleus-dependent transcriptional functions of TSC2, thus expanding its role beyond cytoplasmic signalling regulation and underscoring its significance in the cellular signalling networks.

Introduction

Communication and coordination among different cellular populations are necessary for maintaining homeostasis [1]. In this context, signal transduction pathways act as a molecular language to regulate communication across neighbouring as well as distant cell populations [1]. TSC2 (Tuberous sclerosis complex subunit 2) or tuberin is a critical cell growth suppressor and a major inhibitor of the PI3K-AKT-MTOR signalling pathway [2]. The PI3K-AKT-MTOR axis, also referred to as the cell survival pathway, is a multi-step signal transduction cascade that regulates diverse cellular processes, including cellular growth, survival, proliferation, biomolecule synthesis, metabolism, and apoptosis [3,4]. The canonical PI3K-AKT-MTOR pathway occurs outside the nucleus, primarily in the cytoplasm and lysosomal membrane [3]. However, in addition to their canonical functions, several pathway-associated signalling molecules, including TSC2, are known to translocate into the nucleus, where they contribute to non-canonical nuclear functions [4,5]. The primary role of TSC2 is to suppress MTORC1 activity [6]. The loss of *TSC2* results in MTORC1 hyperactivation and aberrant cellular growth, due to which *TSC2* is also characterized as a classical tumour suppressor gene [2].

TSC2 is located on chromosome 16p13.3 and translates to an 1,807 aa (amino acids) long protein of ~200 kDa (https://www.ncbi.nlm.nih.gov/) [2]. In addition to its presence in the cytoplasm and nucleus, TSC2 also resides in mitochondria, lysosome, and the Golgi apparatus, although its compartment-specific functions are not yet clear [4,7–9]. In the cytoplasm, TSC2 functions as a part of a heteromeric protein complex, widely known as the TSC (tuberous sclerosis complex), along with TSC1 (Tuberous sclerosis complex subunit 1 or hamartin) and TBC1D7 (Tre2-Bub2-CDC16 domain family member 7) subunits [2,10]. TSC2 is the largest and catalytic component of the complex and is composed of one leucine zipper domain (LZ; aa 75-107), two coiled-coil domains (CCs; aa 346-371 and 1008-1021), two transcription activation domains (TADs; aa 1163-1259 and aa 1690-1743), one GTPase activating protein homology domain (GAP; aa 1517-1674), and one nuclear localization signal sequence (NLS; aa 1743-1755) [4]. Mutations and downregulation of *TSC1* and *TSC2* have been observed in several cancers, leading to hyperactivation of MTORC1 signalling and thereby aiding in cancer progression [2]. The mutations in *TSC1* and *TSC2* genes also cause tuberous sclerosis complex disease, an autosomal dominant genetic disorder characterized by the formation of benign tumours (hamartomas) in several organs, including the brain, heart, skin, kidneys, and lungs [11].

The canonical function of TSC2 is to inhibit the PI3K-AKT-MTOR pathway through RHEB (Ras homolog enriched in brain) hydrolysis [6]. TSC2 functions as a GAP (GTPase-activating protein) for its small GTPase, RHEB, and converts RHEB to its inactive GDP-bound form, rendering MTORC1 inactive [6,12]. Apart from its canonical role, TSC2 also exerts cell growth-suppressive effects via MTORC1-independent signalling mechanisms [13]. Although TSC2 is canonically part of the TSC assembly, it can carry out non-canonical functions on its own, independent from the complex [13]. A detailed account of the non-canonical, nuclear-independent functions of TSC2 has been reviewed by Neuman and team [13].

Interestingly, TSC2 has been found in the nucleus of many cell types, including HeLa, HEK293, Rat-1, and NIH3T3, suggesting its ubiquitous nuclear translocation [5]. TSC2 utilizes a 13 aa-long NLS sequence near its C-terminus (RLRHIKRLRQRIR; aa 1743-1755) for its nuclear localization [14]. In another report, Clements and team showed that the deletion of aa positions 1351-1807 from the TSC2 protein reduces its nuclear entry in HASM cells [8]. Moreover, TSC2 nuclear localization is a phosphorylation-dependent process. The phosphorylation of TSC2 at Ser939 and Thr1462 by AKT inhibits TSC2 nuclear entry and retains it in the cytoplasm [15]. In the nucleus, TSC2 acts as a nuclear receptor co-regulator for the steroid receptor family [16,17]. TSC2 enhances transcription driven by the VDR (vitamin D receptor) and PPAR (peroxisome proliferator-activated receptor), while repressing transcriptional activity mediated by the glucocorticoid receptor and ERα (estrogen receptor alpha) [14,16]. In 2014, our research group found the first evidence of a direct nuclear function of TSC2 as a transcription factor [18]. This study demonstrated that the nuclear TSC2 binds directly to the promoter of the oncogene *EREG* (Epiregulin) and represses its expression [18]. The study confirmed the direct binding between TSC2 and the *EREG* promoter by ChIP (chromatin immunoprecipitation) and EMSA (electrophoretic mobility shift assay) experiments, establishing TSC2 as a transcriptional repressor of *EREG* [18]. It is a well-accepted premise that *EREG* is unlikely to be the only gene transcriptionally regulated by TSC2. Given the complex role of TSC2 in cellular signalling, it is highly plausible that TSC2 modulates the transcription of multiple other protein-coding as well as non-coding genes. The present study explored the TSC2-mediated regulation of miRNA (microRNA) genes and the mechanisms underlying its regulation.

MiRNAs are a class of small, non-coding, endogenous, regulatory RNA molecules ranging from 18-25 nucleotides in length [19]. The role of miRNAs in gene regulation is vital for proper development, cell proliferation, survival, and maintenance of normal cellular

physiology [19]. Like protein-coding genes, the transcriptional regulation of miRNAs also occurs directly or indirectly via binding of transcription factors to their gene promoters [20]. This study establishes TSC2 as a transcription factor for a non-coding RNA genes for the first time, and the candidate miRNA uncovers a novel regulatory pathways via epigenetic regulation.

Results

Identification of TSC2 as a negative regulator of miR-514b-3p expression

To identify the TSC2-mediated differentially regulated miRNAs, we silenced TSC2 in SCC131 cells, a human OSCC (oral squamous cell carcinoma) cell line, using a pool of four TSC2-targeting siRNAs, followed by genome-wide miRNA profiling. To this end, we transiently transfected SCC131 cells with Mock and TSC2 siRNAs pools separately. We first confirmed the TSC2 knockdown at both the mRNA and protein levels (Fig. 1A). As *EREG* is a well-established transcriptional target of TSC2, we assessed its expression following TSC2 knockdown. Consistent with the previous report [18], TSC2 silencing resulted in a significant upregulation of *EREG* mRNA levels in TSC2 siRNAs-transfected cells compared to those transfected with Mock siRNAs (Fig. S1). Hence, *EREG* served as a positive control. For genome-wide miRNA profiling, small RNA-enriched fractions were isolated from both Mock and TSC2 siRNAs-transfected cells and subjected to sequencing on a SurePrint G3 8×60K Human miRNA microarray platform, having 2,549 mature miRNA probes (Agilent Technologies, Santa Clara, CA, USA). The miRNA microarray analysis identified a total of 43 differentially regulated miRNAs post TSC2 knockdown, of which 19 miRNAs were significantly upregulated, and 24 miRNAs were significantly downregulated in cells transfected with TSC2 siRNAs as compared to those transfected with Mock siRNAs (Fig. 1B; Table S1). A heat map representing the differentially regulated miRNAs is shown in Fig. 1B and Fig. S2.

Given the established role of TSC2 as a transcriptional repressor of *EREG,* we hypothesized that miRNAs which show upregulation following TSC2 knockdown might be the transcriptional targets of TSC2. Of the 19 upregulated miRNAs, hsa-miR-514b-3p (miR-514b-3p) emerged as one of the most robustly upregulated candidates, exhibiting ~28.5-fold increase in expression (mean log2 fold change of 4.91) in TSC2-silenced cells as compared to those transfected with the Mock siRNAs (Fig. 1B, Table S1). Owing to its strong upregulation following TSC2 knockdown and lack of prior information regarding its transcriptional

regulation, miR-514b-3p was selected as a potential target of TSC2 and subjected to further investigation. The upregulation of miR-514b-3p post TSC2 knockdown was validated by RT-qPCR and RT-PCR using RT6-miR-514b-3p and shortmiR-514b-3p primers (Fig. 1C, Fig. S3, Table S2). The results showed a significant upregulation in miR-514b-3p expression in TSC2 siRNAs-transfected cells as compared to those transfected with the Mock siRNAs, validating the miRNA microarray data (Fig. 1C, Fig. S3). These results suggest that TSC2 negatively regulates miR-514b-3p expression and identify miR-514b-3p as a potential downstream target of TSC2-mediated transcription events.

TSC2 negatively regulates miR-514b-3p expression in an NLS-dependent manner

To determine whether TSC2-mediated repression of miR-514b-3p is dependent on its nuclear localization, we analyzed the miR-514b-3p expression following ectopic expression of wild-type TSC2 ORF (pTSC2) or an NLS-deleted TSC2 ORF (pTSC2-NLSdel) constructs in SCC131 cells. Previous studies have demonstrated that TSC2 enters the nucleus via utilizing an NLS sequence near its C-terminus, and deletion of this sequence restricts its nuclear entry [14]. We first validated NLS-dependent subcellular localization of TSC2 by performing nuclear-cytoplasmic fractionation of SCC131 cells transfected with pcDNA3.1(+), pTSC2, or pTSC2-NLSdel. Consistent with earlier reports [8,14], we also observed a marked reduction in nuclear TSC2 levels in cells transfected with pTSC2-NLSdel as compared to those transfected with pTSC2 (Fig. 1D). The cytoplasmic TSC2 levels remained comparable in cells transfected with pTSC2 and pTSC2-NLSdel constructs (Fig. 1D). These observations confirm that the deletion of NLS from TSC2 ORF effectively impairs the entry of TSC2 to the nucleus without substantially affecting its cytoplasmic presence.

We next examined miR-514b-3p levels in SCC131 cells transfected with pcDNA3.1(+), pTSC2, or pTSC2-NLSdel. As expected, we observed a significantly reduced level of miR-514b-3p in pTSC2-transfected cells as compared to those transfected with the pcDNA3.1(+), confirming the negative regulation of miR-514b-3p by TSC2 (Fig. 1E, Fig. S3). Interestingly, the level of miR-514b-3p showed a significant increase in cells transfected with pTSC2-NLSdel as compared to those transfected with pTSC2 (Fig. 1E). These findings suggest that the presence of TSC2 inside the nucleus is required for modulating the level of miR-514b-3p, thereby establishing miR-514b-3p regulation as a function of nuclear TSC2. Efficient TSC2 overexpression in both pTSC2 and pTSC2-NLSdel conditions was confirmed by checking the TSC2 mRNA levels in both groups (Fig. 1F).

TSC2 acts as a transcriptional repressor for *MIR514B*

Given that TSC2 is a known transcriptional repressor of *EREG*, we speculated whether TSC2 regulates miR-514b-3p at the transcriptional level in a similar manner. Since the promoter region of the *MIR514B* gene has not been previously characterized, we first retrieved the putative promoter sequence of 2,825 bp (-2,575 to + 250 bp relative to the transcription start site; Fig. S4A, S4B) using bioinformatics tools {viz., DBTSS (https://dbtss.hgc.jp/) and Promoter 2.0 (https://services.healthtech.dtu.dk/services/Promoter-2.0/)}, and then functionally validated the cloned fragment pPROM-MIR514B by dual-luciferase reporter assay in SCC131 cells. The results showed a significant luciferase activity in cells transfected with pPROM-MIR514B as compared to those transfected with the pGL3-Basic vector (Fig. 2A), suggesting that the putative sequence exhibits promoter activity and represents the *MIR514B* gene promoter. After *MIR514B* promoter characterization, we aimed to examine the effect of pTSC2 and pTSC2-NLSdel on the *MIR514B* promoter (pPROM-MIR514B) activity by the dual-luciferase reporter assay. To this end, we transfected SCC131 cells with pPROM-MIR514B alone, co-transfected with pPROM-MIR514B and different quantities of pTSC2 (i.e., 200 ng, 400 ng, and 600 ng), or co-transfected with pPROM-MIR514B and pTSC2-NLSdel. The subsequent results showed concomitant reduction in luciferase activity in cells co-transfected with pPROM-MIR514B and different quantities of pTSC2 in a dose-dependent manner as compared to those transfected with pPROM-MIR514B only, suggesting that TSC2 negatively regulates the *MIR514B* promoter activity (Fig. 2B). Furthermore, the luciferase activity significantly increased in cells co-transfected with pPROM-MIR514B and pTSC2-NLSdel as compared to those co-transfected with pPROM-MIR514B and pTSC2, suggesting that TSC2 negatively regulates the *MIR514B* promoter activity in a nucleus-dependent manner (Fig. 2B). Similar results have been observed in cells from another OSCC cell line, SCC084 (Fig. S4C).

To determine whether TSC2 acts as a transcriptional repressor of *MIR514B* by directly binding its promoter, we performed ChIP-qPCR analysis. Previous research from our group had identified a putative TBS (TSC2 binding site; 5' GCCTTG 3') in the promoters of several TSC2-regulated genes [18]. We therefore looked for this putative TBS in the characterized *MIR514B* promoter near the TSS and found seven partial TSC2 binding sites: TBS1-TBS7 (Fig. S5A, S5B). We designed separate PCR primers across all seven potential TBSs and amplified them individually by ChIP-qPCR, using DNA isolated from TSC2 and IgG pull-down samples (Table S3). The subsequent ChIP-qPCR analysis showed a strong TSC2

enrichment at five out of seven TBSs in the *MIR514B* promoter (viz., TBS2, TBS3, TBS4, TBS5, and TBS6 in the TSC2 pull-down sample as compared to the IgG pull-down sample, confirming the direct interaction between TSC2 and *MIR514B* promoter (Fig. 2C). However, TBS1 did not show any TSC2 enrichment, whereas TBS7 did not show any amplification in ChIP-qPCR (Fig. 2C). As expected, a strong TSC2 enrichment was observed at the *EREG* promoter in the TSC2 pull-down sample as compared to the IgG pull-down sample (Fig. 2C). A H3-ChIP was also performed which served as an internal positive control (Fig. S5C). The TSC2 enrichment at multiple sites in the *MIR514B* promoter confirms the direct binding of TSC2 to the *MIR514B* promoter. Hence, TSC2 acts as a transcriptional repressor, binds directly to the *MIR514B* promoter, and negatively regulates miR-514b-3p expression.

***TSPAN9* is a direct gene target of miR-514b-3p**

The miRNAs bind to their cognate target mRNAs via sequence complementarity to regulate their gene expression. To find out the direct gene targets of miR-514b-3p, we employed five miRNA prediction tools and obtained five putative miR-514b-3p targets: *TSPAN9* (Tetraspanin 9), *PTEN* (Phosphatase and Tensin Homolog deleted on chromosome 10), *GULP1* (GULP PTB Domain Containing Engulfment Adaptor 1), *SESN3* (Sestrin 3), and *CABLES1* (Cdk5 and Abl Enzyme Substrate 1) (Table S4). For preliminary analysis, we examined expression of these putative targets in an miR-514b-3p overexpression background and observed that, of the five targets, *TSPAN9* showed the most extent of downregulation in cells transfected with pMIR514B as compared to those transfected with the pcDNA3-EGFP (Fig. S6A). The other predicted targets showed no or only marginal change, whereas the known target of miR-514b-3p, *RBX* (Ring-box 1), showed significant downregulation post miR-514b-3p overexpression (Fig. S6B-6F) [21]. Next, we transiently transfected SCC131 cells with pMIR514B and pcDNA3-EGFP separately and determined the transcript and protein levels of TSPAN9. The results showed a marked reduction in TSPAN9 levels in cells transfected with pMIR514B compared to those transfected with the pcDNA3-EGFP, suggesting miR-514b-3p negatively regulates both the transcript and protein levels of TSPAN9 (Fig. 3A). To confirm this observation further, we performed a dose-dependent transient transfection of SCC131 cells with different quantities of the pMIR514B construct (viz., 2µg, 4µg, and 6µg) and pcDNA3-EGFP separately and determined transcript and protein levels of TSPAN9. The results showed a concomitant reduction in TSPAN9 transcript and protein levels with increasing levels of miR-

514b-3p, suggesting a dose-dependent negative regulation of TSPAN9 by miR-514b-3p (Fig. 3B).

Our bioinformatics analysis predicted a putative TS (target site) for miR-514b-3p binding in the 3'UTR of *TSPAN9,* spanning nucleotides 3432-3439, which is conserved across species (Fig. S7A). We performed a dual-luciferase reporter assay to confirm the direct interaction between the SR (seed region) of miR-514b-3p and the TS in the 3'UTR of *TSPAN9*, using constructs illustrated in Fig. S7B. The p3'UTR-TSPAN9 construct harbours *TSPAN9* 3'UTR in sense orientation with the intact TS, whereas the p3'UTR-TSPAN9-M construct is generated by abrogating the TS for miR-514b-3p in the 3'UTR of *TSPAN9* by site-directed mutagenesis (Fig. S7B). To determine whether miR-514b-3p directly interacts with TS present in *TSPAN9* 3'UTR, we co-transfected SCC131 cells separately with p3'UTR-TSPAN9 and pcDNA3-EGFP, p3'UTR-TSPAN9 and pMIR514B, or p3'UTR-TSPAN9-M and pMIR514B and performed a dual-luciferase reporter assay. Compared to cells co-transfected with p3'UTR-TSPAN9 and pcDNA3-EGFP, we observed a significant decrease in the luciferase activity in those co-transfected with p3'UTR-TSPAN9 and pMIR514B, confirming that miR-514b-3p binds directly to the 3'UTR of *TSPAN9* (Fig. 3C). Moreover, cells co-transfected with p3'UTR-TSPAN9-M and pMIR514B showed the luciferase activity comparable to those co-transfected with p3'UTR-TSPAN9 and pcDNA3-EGFP, due to the absence of miR-514b-3p TS in the p3'UTR-TSPAN9-M construct (Fig. 3C). These observations confirm that the miR-514b-3p binds directly to the TS present in the *TSPAN9* 3'UTR in a sequence-specific manner. Hence, *TSPAN9* is a direct gene target of miR-514b-3p. We also observed direct interaction between miR-514b-3p and *RBX* 3'UTR, which served as a positive control for the assay (Fig. 3C).

miR-514b-3p negatively regulates TSPAN9 protein levels by interacting with its 3'UTR

We demonstrated that miR-514b-3p negatively regulates TSPAN9 expression and exhibits direct binding to *TSPAN9* 3'UTR in a sequence-specific manner. To unequivocally show that the binding between miR-514b-3p and *TSPAN9* 3'UTR downregulates TSPAN9 expression, we performed Western blot analysis with the following constructs: pTSPAN9 (harbours *TSPAN9* ORF), pTSPAN9-3'UTR (harbours *TSPAN9* ORF and its 3'UTR with a functional TS for miR-514b-3p), and pTSPAN9-3'UTR-M (harbours TSPAN9 ORF and its 3'UTR after abrogation of TS for miR-514b-3p) (Fig. S7C). We transiently transfected SCC131 and SCC084 cells with pcDNA3.1(+) only or co-transfected with pcDNA3.1(+) and pMIR514B, pTSPAN9 and pMIR514B, pTSPAN9-3'UTR and pMIR514B, or pTSPAN9-

3'UTR-M and pMIR514B and subsequently determined TSPAN9 protein levels. The results showed that, as compared to cells transfected with pcDNA3.1(+) only, cells co-transfected with pcDNA3.1(+) and pMIR514B showed a decreased level of TSPAN9, due to targeting of the endogenous TSPAN9 by miR-514b-3p (Fig. 3D, Fig. S7D). Further, TSPAN9 levels were increased in cells co-transfected with pTSPAN9 and pMIR514B as compared to those co-transfected with pcDNA3.1(+) and pMIR514B, due to the TSPAN9 overexpression by pTSPAN9 (Fig. 3D, Fig. S7D). Furthermore, the cells co-transfected with pTSPAN9-3'UTR and pMIR514B showed a marked reduction in the TSPAN9 levels as compared to those transfected with pTSPAN9 and pMIR514B, due to the presence of a functional TS in the pTSPAN9-3'UTR, resulting in the interaction between *TSPAN9* 3'UTR and miR-514b-3p (Fig. 3D, Fig. S7D). Moreover, the TSPAN9 levels in cells co-transfected with pTSPAN9-3'UTR-M and pMIR514B were comparable to those transfected with pTSPAN9 and pMIR514B, due to the abrogation of TS in pTSPAN9-3'UTR-M (Fig. 3D, Fig. S7D). These observations confirm that the negative regulation of TSPAN9 by miR-514b-3p is dependent on the presence or absence of its 3'UTR.

TSC2 positively regulates *TSPAN9* expression via TSC2-miR-514b-3p-TSPAN9 axis

Since TSC2 negatively regulates miR-514b-3p, which in turn negatively regulates *TSPAN9*, it is reasonable to assume that TSC2 might positively regulate *TSPAN9* expression. To this end, we performed TSC2 knockdown and TSC2 overexpression in SCC131 cells. As expected, we observed a sharp reduction in the TSPAN9 expression at both transcript and protein levels in cells transfected with TSC2 siRNAs compared to those transfected with the Mock siRNAs (Fig. 4A). Furthermore, TSPAN9 was upregulated in cells transfected with pTSC2 compared to those transfected with pcDNA3.1(+), suggesting TSC2-mediated positive regulation of TSPAN9 at both the transcript and protein levels (Fig. 4B). Moreover, the TSPAN9 expression in pTSC2-NLSdel-transfected SCC131 cells was comparable to those transfected with pcDNA3.1(+), suggesting TSC2-mediated NLS-dependent regulation of TSPAN9 expression (Fig. 4B). These observations suggest the existence of a nucleus-dependent TSC2-miR-514b-3p-TSPAN9 axis.

TSC2 and TSPAN9 are anti-proliferative, whereas miR-514b-3p is pro-proliferative in nature

After establishing the TSC2-miR-514b-3p-TSPAN9 axis, we aimed to examine the independent effects of each of these molecules on the proliferation of OSCC cells. We

separately transfected OSCC cells with pTSC2, pTSPAN9, and pMIR514B constructs along with appropriate vectors and assessed proliferation using trypan blue dye exclusion and BrdU cell proliferation assays. The trypan blue dye exclusion assay showed a significantly reduced proliferation of OSCC cells transfected with pTSC2 or pTSPAN9 as compared to those transfected with pcDNA3.1(+), suggesting the anti-proliferative nature of TSC2 and TSPAN9 (Fig. 5A,B; Fig. S8A,B). Further, we observed a significant increase in the proliferation of OSCC cells transfected with pMIR514B compared to those transfected with pcDNA3-EGFP, indicating the pro-proliferative nature of miR-514b-3p (Fig. 5C, Fig. S8C). The BrdU cell proliferation assay also showed a significant reduction in absorbance in OSCC cells transfected with pTSC2 or pTSPAN9 as compared to those transfected with pcDNA3.1(+), confirming the anti-proliferative nature of TSC2 and TSPAN9 (Fig. 5D,E; Fig. S8D,E). Further, we observed a significant increase in absorbance in OSCC cells transfected with pMIR514B as compared to those transfected with pcDNA3-EGFP, confirming the pro-proliferative nature of miR-514b-3p (Fig. 5F, Fig. S8F).

miR-514b-3p regulates the proliferation, apoptosis, and anchorage-independent growth of OSCC cells, in part, by targeting the 3'UTR of *TSPAN9*

To determine if miR-514b-3p regulates different hallmarks of cancer, by targeting the *TSPAN9* 3'UTR, we transiently transfected SCC131 and SCC084 cells with different constructs in the following combinations: pcDNA3.1(+) only, pcDNA3.1(+) and pMIR514B, pTSPAN9 and pMIR514B, pTSPAN9-3'UTR and pMIR514B, or pTSPAN9-3'UTR-M and pMIR514B and performed functional assays.

We examined proliferation of OSCC cells by trypan blue dye exclusion and BrdU cell proliferation assay, and results showed that cells co-transfected with pcDNA3.1(+) and pMIR514B showed enhanced cell proliferation as compared to those transfected with only pcDNA3.1(+), indicating the pro-proliferative nature of miR-514b-3p (Fig. 6A, Fig. S9A). The cells co-transfected with pTSPAN9-3'UTR and pMIR514B showed increased cell proliferation as compared to those transfected with pTSPAN9 and pMIR514B, as well as pTSPAN9-3'UTR-M and pMIR514B, due to the functional TS in pTSPAN9-3'UTR (Fig. 6A, Fig. S9A). Moreover, the proliferation of cells co-transfected with pTSPAN9-3'UTR-M and pMIR514B was comparable to those co-transfected with pTSPAN9 and pMIR514B, due to the absence of a functional TS in pTSPAN9-3'UTR-M (Fig. 6A, Fig. S9A). Similar results were observed by the BrdU cell proliferation assay in both cell lines (Fig. 6B, Fig. S9B). These observations

clearly suggest that miR-514b-3p positively regulates the proliferation of OSCC cells, in part, by targeting the 3'UTR of *TSPAN9.*

We next examined apoptosis of OSCC cells by the Caspase-3 activation assay. The results demonstrated that the cells co-transfected with pcDNA3.1(+) and pMIR514B showed reduced Caspase-3 activity as compared to those transfected with only pcDNA3.1(+), indicating the anti-apoptotic nature of miR-514b-3p (Fig. 6C, Fig. S9C). The cells co-transfected with pTSPAN9-3'UTR and pMIR514B showed reduced Caspase-3 activity as compared to those transfected with pTSPAN9 and pMIR514B as well as pTSPAN9-3'UTR-M and pMIR514B, due to a functional TS in pTSPAN9-3'UTR (Fig. 6C, Fig. S9C). Moreover, the Caspase-3 activity in cells co-transfected with pTSPAN9-3'UTR-M and pMIR514B was comparable to those co-transfected with pTSPAN9 and pMIR514B, due to the absence of a functional TS in *TSPAN9* 3'UTR in pTSPAN9-3'UTR-M (Fig. 6C, Fig. S9C). The above observations suggest that miR-514b-3p negatively regulates apoptosis of OSCC cells, in part, by targeting the 3'UTR of *TSPAN9.*

To study the anchorage-independent growth of OSCC cells, we performed a soft agar colony formation assay and observed that cells co-transfected with pcDNA3.1(+) and pMIR514B showed enhanced colony formation as compared to those transfected with only pcDNA3.1(+), indicating a pro-proliferative nature of miR-514b-3p (Fig. 6D, Fig. S9D). The cells co-transfected with pTSPAN9-3'UTR and pMIR514B showed an increased number of colonies as compared to those transfected with pTSPAN9 and pMIR514B, as well as pTSPAN9-3'UTR-M and pMIR514B, due to the functional TS in pTSPAN9-3'UTR (Fig. 6D, Fig. S9D). Moreover, the number of colonies in cells co-transfected with pTSPAN9-3'UTR-M and pMIR514B was comparable to those co-transfected with pTSPAN9 and pMIR514B, due to the absence of a functional TS in pTSPAN9-3'UTR-M (Fig. 6D, Fig. S9D). Thus, the miR-514b-3p-mediated inhibition of *TSPAN9* leads to enhanced anchorage-independent growth of OSCC cells due to the pro-proliferative nature of miR-514b-3p, suggesting miR-514b-3p positively regulates the anchorage-independent growth of OSCC cells, in part, by targeting the 3'UTR of *TSPAN9.*

The miR-514b-3p-TSPAN9 axis regulates the PI3K-AKT-MTOR pathway via nucleus

TSC2 is a well-established suppressor of the PI3K-AKT-MTOR pathway. As we have demonstrated that the regulation of miR-514b-3p/TSPAN9 is a nuclear function of TSC2, we

were interested to know if the downstream targets of the nuclear TSC2 (viz., miR-514b-3p and TSPAN9) can also regulate the canonical PI3K-AKT-MTOR pathway. To this end, we overexpressed miR-514b-3p and TSPAN9 along with their appropriate vectors in OSCC cells and analyzed the PI3K-AKT-MTOR pathway readout by checking the phospho-S6K1 (Thr389) (pS6K1) and total S6K1 levels. We also analyzed the levels of crucial mediators such as PI3K (p55), phospho-AKT (Ser473) (pAKT), and total AKT. Following miR-514b-3p overexpression, we observed increased levels of pS6K1, p55, and pAKT in OSCC cells transfected with pMIR514B as compared to those transfected with pcDNA3-EGFP, suggesting that miR-514b-3p positively regulates the PI3K-AKT-MTOR pathway (Fig. 7A). The total S6K1 and total AKT levels remained similar in both samples (Fig. 7A). As expected, TSPAN9 level exhibited a marked decrease in cells transfected with pMIR514B as compared to those transfected with the pcDNA3-EGFP due to miR-514b-3p-mediated TSPAN9 inhibition (Fig. 7A).

Furthermore, we observed decreased levels of pS6K1, p55, and pAKT in cells transfected with pTSPAN9 as compared to those transfected with pcDNA3.1(+), suggesting that TSPAN9 negatively regulates the PI3K-AKT-MTOR pathway (Fig. 7B). The total S6K1 and total AKT levels remained similar in both samples (Fig. 7B). It is important to note that the activation of the PI3K-AKT-MTOR pathway is widely known to enhance cell proliferation. Our observations thus align well with the pro-proliferative nature of miR-514b-3p and the anti-proliferative nature of *TSPAN9* (Fig. 5, Fig. S8). These observations therefore suggest that miR-514b-3p is a positive regulator, whereas TSPAN9 is a negative regulator of the PI3K-AKT-MTOR pathway.

AKT modulates the TSC2-miR-514b-3p-TSPAN9 axis via TSC2 nuclear localization

The phosphorylation of TSC2 by AKT at Ser939 and Thr1462 leads to its inactivation and proteasomal degradation [22]. Interestingly, AKT phosphorylation is also crucial for TSC2 nuclear-cytoplasmic shuttle dynamics, where the AKT-mediated inactivating phosphorylation of TSC2 reduces its nuclear entry [22]. To understand the role of AKT in TSC2 nuclear localization in our model system and its effect on the TSC2-miR-514b-3p-TSPAN9 axis, we have used AKT inhibitor VIII (AKTi) to inactivate AKT activity in SCC131 and SCC084 cells. Our hypothesis was based on the premise that the AKT inactivation should drive more TSC2 to the nucleus, which might further inhibit miR-514b-3p expression transcriptionally, and thus enhance TSPAN9 levels.

To confirm the AKT-mediated nuclear localization of TSC2, we performed nuclear-cytoplasmic fractionation of AKTi and vehicle-treated OSCC cells, followed by Western blot analysis. The results showed increased levels of nuclear TSC2 in AKTi-treated cells as compared to those treated with the vehicle (DMSO), whereas the cytoplasmic pool of TSC2 remained unchanged in both treatments (Fig. 8; upper panels).

The Western blot analysis of AKTi and vehicle-treated OSCC cells showed a sharp reduction in pAKT Ser473 and pTSC2 Ser939 levels in AKTi-treated cells compared to vehicle-treated cells, indicating effective inhibition of AKT signalling by AKT inhibitor VIII (Fig. 8; upper panels). The total AKT and total TSC2 levels remained unchanged in both treatments (Fig. 8; upper panels). Interestingly, we observed a significant reduction in miR-514b-3p expression in AKTi-treated cells as compared to those treated with vehicle, suggesting nuclear TSC2-mediated inhibition of miR-514b-3p (Fig. 8; lower panels). Furthermore, we observed elevated TSPAN9 levels in AKTi-treated cells compared with vehicle-treated cells, suggesting miR-514b-3p-mediated *TSPAN9* regulation (Fig. 8; upper and lower panels). These findings clearly demonstrates that AKT regulates miR-514b-3p/TSPAN9 axis via modulating TSC2 nuclear localization.

Inhibition of MTORC1 does not affect the TSC2-miR-514b-3p-TSPAN9 axis

To rule out the possibility that TSC2 can regulate the miR-514b-3p-TSPAN9 axis indirectly via cytoplasm, we decided to inhibit MTORC1 (the primary downstream target of TSC2 in the cytoplasm) by treating OSCC cells with rapamycin and vehicle (DMSO) separately and examined its effect on the levels of miR-514b-3p and TSPAN9. As expected, we observed a sharp reduction in pS6K1 levels in rapamycin-treated cells as compared to those treated with the vehicle, indicating an effective MTORC1 inhibition (Fig. 9; upper panels). Further, we observed that the levels of miR-514b-3p and TSPAN9 remained unaltered in rapamycin and vehicle-treated cells, suggesting that TSC2-mediated regulation of the miR-514b-3p/TSPAN9 axis is rapamycin-insensitive and hence independent of its MTORC1 function (Fig. 9; upper and lower panels).

Discussion

The present study demonstrates that TSC2 negatively regulates miR-514b-3p expression as a transcriptional repressor. In 1998, Henry et al. demonstrated that TSC2 acts as a nuclear receptor co-regulator and mediates the transcriptional events led by the steroid

receptor superfamily in a bidirectional manner [16]. Specifically, TSC2 positively regulates the transcription mediated by VDR and PPRα, while repressing transcription mediated by the glucocorticoid receptor and ERα [16]. The direct interaction of TSC2 with VDR and ERα points towards its role as a nuclear receptor co-regulator [14,16].

The subsequent work from our laboratory identified *EREG* as the first transcriptional target of TSC2, demonstrating that TSC2 binds directly to the *EREG* promoter and suppresses its transcription [18]. While *EREG* represents a prototypical TSC2-regulated gene, it is unlikely to be the sole transcriptional target of TSC2. Given its nuclear localization and interaction with transcriptional machinery, it is reasonable to speculate that TSC2 regulates a broader repertoire of both coding and non-coding genes. In this context, Ogórek et al. reported widespread alterations in miRNA expression following TSC2 loss in mouse embryonic fibroblasts, identifying 161 differentially expressed miRNAs, demonstrating the role of TSC2 in miRNA biogenesis [23]. However, this study attributed TSC2-mediated miRNA biogenesis to a cytoplasmic function of TSC2, mediated through the MTORC1 pathway [23]. In contrast, we sought to delineate the role of nuclear TSC2 in transcriptional regulation, with a particular focus on identifying miRNA genes that are regulated by TSC2 at the transcriptional level.

Our miRNA microarray analysis in SCC131 cells transfected with TSC2 siRNAs and Mock siRNAs led to the identification of 19 upregulated and 24 downregulated miRNAs, of which miR-514b-3p was one of the most robustly upregulated miRNAs (Fig. 1B; Fig. S2; Table S1). The miR-514b-3p is encoded by the *MIR514B* gene located at chromosome Xq27.3 within an intergenic region, suggesting transcription from an independent promoter. (UCSC Genome browser; https://genome.ucsc.edu/). Previous studies have reported context-dependent roles of miR-514b-3p in cancer, functioning either as an oncogene or a tumour suppressor [21,24–27]. Notably, miR-514b-3p has been shown to exert oncogenic functions in gastric cancer and tumour mycosis fungoides, where its expression is elevated [24,26]. Our observation of TSC2-mediated negative regulation of miR-514b-3p is consistent with these reports and suggests a putative oncogenic role for miR-514b-3p in OSCC cells [24,26] (Fig. 1C,E).

Given that TSC2 represses *EREG* transcription via nucleus, we hypothesized that miR-514b-3p regulation might similarly depend on nuclear TSC2. York et al. demonstrated that TSC2 enters the nucleus via utilizing its NLS sequence near the C-terminus, and deletion of this sequence restricts TSC2 nuclear entry [14]. By selectively disrupting this NLS, we show that miR-514b-3p expression is significantly elevated in cells expressing the NLS-deleted

TSC2 mutant compared with cell expressing wild-type TSC2, suggesting that TSC2 negatively regulates miR-514b-3p levels in an NLS-dependent manner (Fig. 1D,E; Fig. S3). The deletion of NLS from the TSC2 suppresses the entry of exogenous TSC2 into the nucleus and results in hampering TSC2-mediated miR-514b-3p regulation.

To elucidate the underlying mechanism, we examined whether TSC2 directly regulates miR-514b-3p transcription by binding to the *MIR514B* promoter. Given the absence of neighbouring genes within a >10 Mbp region, it is likely that *MIR514B* expression is driven by its own independent promoter. Using a dual-luciferase reporter assay, we characterized the *MIR514B* promoter and demonstrated that TSC2 represses *MIR514B* promoter activity in a dose-dependent and NLS-dependent manner (Fig. 2A,B; Fig. S4C). This mode of regulation closely mirrors the previously described TSC2-mediated repression of the *EREG* promoter [18]. Further sequence analysis revealed the presence of seven putative TSC2 binding sites (TBSs) within the *MIR514B* promoter (Fig. S5A,B). The subsequent ChIP-qPCR analysis confirmed the direct binding of TSC2 to the five out of seven TBSs (TBS2, TBS3, TBS4, TBS5, and TBS6) in the *MIR514B* promoter, providing definitive evidence that TSC2 physically associates with the *MIR514B* promoter to repress its transcription (Fig. 2C). Notably, miR-514b-3p is the first identified non-coding (second overall after *EREG*) transcriptional target of TSC2. Hence, nuclear TSC2 exerts its transcriptional function by binding to the promoter of its target genes, *EREG* and *MIR514B*, and negatively regulates their expression.

MiRNAs exert their downstream effects by interacting with the TS (target site) located within 3'UTR, 5'UTR, coding region, and regulatory elements of their mRNA targets [28]. Given that *TSC2* is a classical tumour suppressor gene that negatively regulates miR-514b-3p expression, we sought to identify a downstream target of miR-514b-3p with a tumor-suppressive function. Through a combination of bioinformatics prediction and experimental validation, we identified *TSPAN9* (Tetraspanin 9) as a direct gene target of miR-514b-3p (Fig. 3, Fig. S6, S7, Table S4). TSPAN9 is a member of the tetraspanin family of proteins, a highly conserved group of transmembrane proteins that facilitate cellular signalling by assembling tetraspanin-enriched microdomains (TEMs) at the plasma membrane [29]. *TSPAN9* has been reported to act as a tumour suppressor in gastric and liver cancers, and as an oncogene in osteosarcoma, underscoring its context-dependent role in different cancers [30–33]. In OSCC cells, we observed a dose-dependent downregulation of TSPAN9 expression upon miR-514b-3p overexpression, indicating miR-514b-3p-mediated inhibition of *TSPAN9* (Fig. 3A,B). Sequence analysis revealed a single TS within the *TSPAN9* 3'UTR (nucleotide positions 3432-

3439, relative to TSS), complementary to the miR-514b-3p seed region (Fig. S7A). The dual-luciferase reporter assay confirmed that SR of miR-514b-3p interacts directly with the TS in the *TSPAN9* 3'UTR in a sequence-specific manner (Fig. 3C). Consistently, Western blot analysis demonstrated that miR-514b-3p suppresses TSPAN9 protein expression through direct binding to its 3'UTR in a sequence-specific manner (Fig. 3D, Fig. S7D). Importantly, deletion of the target site from the *TSPAN9* 3′UTR abolished this interaction, resulting in loss of miR-514b-3p-mediated repression of TSPAN9 (Fig. 3C, Fig. 3D, Fig. S7D).

Functionally, our results demonstrate that miR-514b-3p promotes, whereas *TSPAN9* suppresses, proliferation of OSCC cells, consistent with their respective oncogenic and tumour suppressive roles (Fig. 5, Fig. S8). These findings align with observations in gastric cancer, where miR-514b-3p functions as an oncomiR and *TSPAN9* acts as a tumour suppressor [26,30,31,34]. Furthermore, we show that miR-514b-3p enhances cell proliferation and anchorage-independent growth, while inhibiting apoptosis of OSCC cells, in part, by targeting the *TSPAN9* 3'UTR in a sequence-specific manner (Fig. 6, Fig. S9). It is noteworthy that by suppressing *TSPAN9* expression and hence its tumour suppressor function, miR-514b-3p exhibits its oncogenic properties via regulating these cancer hallmarks. Disruption of the miR-514b-3p-TSPAN9 interaction abrogates these effects, reinforcing the functional relevance of this regulatory interaction in governing key cancer hallmarks (Fig. 6, Fig. S9).

Consistent with its role as a transcriptional repressor of miR-514b-3p, TSC2 positively regulates TSPAN9 expression in an NLS-dependent manner (Fig. 4). Given the direct binding between TSC2 and the *MIR514B* promoter, as well as miR-514b-3p and *TSPAN9*, we reasoned that TSC2 should regulate *TSPAN9* via miR-514b-3p regulation. Thus, tumour suppressor *TSC2* inhibits the oncogenic miR-514b-3p, while miR-514b-3p suppresses the expression of another tumour suppressor, *TSPAN9*, establishing a regulatory axis, TSC2-miR-514b-TSPAN9. Collectively, our study identified a novel, nucleus-mediated TSC2-miR-514b-3p-TSPAN9 axis in OSCC cells.

We next investigated whether this newly found axis intersects with the canonical PI3K-AKT-MTOR pathway in the cytoplasm. TSPAN9 has previously been shown to suppress PI3K-AKT-MTOR signalling by promoting degradation of the PI3K p55 subunit in gastric cancer [31]. In agreement with this mechanism, we observed upregulation of p55, pAKT, and pS6K1 levels following miR-514b-3p overexpression and downregulation of p55, pAKT, and pS6K1 levels following TSPAN9 overexpression in OSCC cells (Fig. 7). The miR-514b-3p

overexpression causes reduced levels of TSPAN9, leading to the upregulation of p55 and subsequent activation of AKT and S6K1 (Fig. 7). Notably, the alteration in TSC2 levels regulates the miR-514b-3p/TSPAN9 axis, whereas alteration in miR-514b-3p/TSPAN9 levels further modulates the PI3K-AKT-MTOR pathway, suggesting the existence of a positive feedback loop (Fig. 7). In addition, the miR-514b-3p-mediated activation and TSPAN9-mediated inhibition of the PI3K-AKT-MTOR pathway further ensure their respective oncogenic and tumour suppressor potential in OSCC cells. This is particularly noteworthy that TSC2 negatively regulates the PI3K-AKT-MTOR pathway via RHEB inhibition in the cytoplasm and as a transcriptional repressor of oncogenes, *EREG* and *MIR514B* via nucleus.

AKT is known to regulate the nuclear-cytoplasmic shuttling of TSC2 through phosphorylation at Ser939 and Thr1462, thereby restricting its nuclear functions [22]. In line with this, pharmacological inhibition of AKT with AKTi (AKT inhibitor VIII) in OSCC cells resulted in downregulation of miR-514b-3p and upregulation of TSPAN9 levels (Fig. 8). These observations can be attributed to the enhanced translocation of TSC2 in the nuclear compartment following AKT inhibition, which leads to transcriptional suppression of miR-514b-3p, resulting in the elevated TSPAN9 levels (Fig. 8). These results further underscore the inter-dependence between the canonical PI3K-AKT-MTOR signalling and the newly identified TSC2-miR-514b-3p-TSPAN9 axis. To enunciate that the regulation of miR-514b-3p/TSPAN9 axis is independent from cytoplasmic role of TSC2, we treated OSCC cells with rapamycin, a widely known inhibitor of the MTORC1 activity [12]. Notably, inhibition of MTORC1 activity did not alter miR-514b-3p and TSPAN9 levels, confirming that the regulation of the miR-514b-3p/TSPAN9 axis is MTORC1-independent and is not a cytoplasmic function of TSC2 (Fig. 9).

Taken together, this study identifies miR-514b-3p as the first non-coding transcriptional target of TSC2 and delineated the molecular mechanism underlying its regulation. The study establishes *TSPAN9* as a downstream target of miR-514b-3p and discovered a novel nucleus-driven TSC2-miR-514b-3p-TSPAN9 axis in OSCC cells. Further research on the oncogenic properties of miR-514b-3p and the tumour suppressor properties of TSPAN9 might benefit therapeutic interventions in OSCC and other malignancies.

Materials and Methods

Plasmid constructs

The details of plasmid constructs generated for the present study are summarized in Table S5. The following constructs viz., pPROM-MIR514B, pMIR514B, p3'UTR-TSPAN9,

p3'UTR-RBX, and pTSPAN9 were generated using human genomic DNA or cDNA as template and gene specific primers (Table S5) by standard laboratory protocols. The p3'UTR-TSPAN9-M was generated by site-directed mutagenesis using specific primers (Table S5). pTSPAN9-3'UTR and pTSPAN9-3'UTR-M were generated by cloning TSPAN9 3'UTR and TSPAN9 3'UTR-M respectively downstream to pTSPAN9. All the constructs were subjected for Sanger sequencing on an ABI PRISM A310-automated sequencer (Thermo Fisher Scientific, Waltham, MA, USA) to confirm directionality and error-free sequences.

Cell culture and transient transfections

Human oral squamous cell carcinoma cell lines, UPCI-SCC-131 and UPCI-SCC-084, were a kind gift from Prof. Susanne M. Gollin, University of Pittsburgh, PA, USA and were generated following institutional review board guidelines from consenting patients undergoing surgery for OSCC. Both of the cell lines were cultured in DMEM (Dulbecco's Modified Eagle Medium, high glucose), supplemented with 10% FBS (Fetal Bovine Serum) and 1X Antibiotic-Antimycotic solution (all from Sigma-Aldrich, St. Louis, MO, USA) at 37ºC in 5% CO_2.

SCC131 or SCC084 cells were seeded at a density of 2×10^6 cells per well in a 6-well plate and transiently transfected with appropriate plasmid construct(s) using Lipofectamine 2000 transfection reagent (Thermo Fisher Scientific, Waltham, MA, USA) per the manufacturer's instructions. After 48 hr, cells were harvested for RNA and protein isolation as per experiment plan.

siRNA mediated TSC2 knockdown

A SMART pool of four siRNAs targeting *TSC2* transcript and a non-targeting pool of four siRNAs (Mock) were commercially purchased from the GE Healthcare Dharmacon, Lafayette, CO, USA (Table S6). SCC131 cells were seeded at a density of 2×10^6 cells per well in a 6-well plate and transiently transfected either with 100 nM Mock siRNAs or TSC2 siRNAs pool separately using Lipofectamine 2000 in SCC131 cells following manufacturer's instructions. After 48 hr, cells were harvested for small RNA, total RNA, and total protein isolation as per experiment plan.

Microarray analysis

The small RNA isolated from Mock and TSC2 siRNAs-transfected cells (3 replicates each) were sent for microRNA microarray analysis (Genotypic technology, Bengaluru, India). The microRNA microarray was performed on SurePrint G3 8 × 60k Human miRNA microarray

platform having 2,549 mature miRNAs probes (AMADID 70156; Agilent Technologies, Santa Clara, CA, USA). The miRNA microarray data was analyzed to find out differentially regulated miRNAs after TSC2 knockdown. A list of differentially regulated miRNAs following TSC2 knockdown is given in Table S1.

Bioinformatics analysis to identify miR-514b-3p targets

We have performed bioinformatics analysis to predict the gene targets for miR-514b-3p. The bioinformatics analysis tools use machine learning algorithms and consider the experimentally validated miRNAs, conservation score, and free energy calculations to predict the possible targets for miRNAs. The bioinformatics tools used for the gene target prediction of miR-514b-3p were Agilent GeneSpring (https://shorturl.at/4dJHb), miRDB [35], TargetScanHuman8.0 [36], microT-CDS [37], and STarMirDB [38].

RNA isolation and cDNA synthesis

The total RNA was isolated using TRI-Reagent per the manufacturer's protocol (Sigma-Aldrich, St. Louis, MO, USA), and quantified using NanoDrop 1000 spectrophotometer (Thermo Fisher Scientific, Waltham, MA, USA). The first-strand cDNA synthesis was performed using Verso cDNA synthesis kit (Thermo Fisher Scientific, Waltham, MA, USA) and 1-2 µg of total RNA as template.

Reverse transcription-quantitative PCR

The transcript level of miR-514b-3p was determined by RT-qPCR-based miR-Q assay [39], whereas for all other transcript level expression were determined by conventional RT-qPCR. The details of the primers are given in Table S2. The RT-qPCR was performed using DyNAmo ColorFlash SYBR Green qPCR kit (Thermo Fisher Scientific, Waltham, MA, USA) in a QuantStudio 3 PCR system (Thermo Fisher Scientific, Waltham, MA, USA) as per the manufacturer's instructions. The RT-qPCR data was analyzed to calculate the relative gene expression using the following formula: $\Delta C_{t\ (gene)} = C_{t\ (gene)} - C_{t\ (normalizing\ control)}$, followed by calculating fold change using $2^{(-\Delta\Delta C_t)}$, where C_t represents the cycle threshold value. 5S *rRNA* and *GAPDH* were used as a normalization controls. Each bar represents the relative fold change expression of a gene of interest normalized to its housekeeping gene and is an average of 3 biological replicates.

Western blot analysis

The total protein was isolated using CelLytic M Cell Lysis reagent (Sigma-Aldrich, St. Louis, MO, USA), resolved on SDS-PAGE, and transferred to a PVDF membrane (Cytiva, Marlborough, MA, USA). The blots were probed with appropriate primary antibodies and visualized by a ChemiDoc imaging system equipped with a CCD camera (Bio-rad, Inc, Hercules, CA, USA) using Immobilon Western chemiluminescent HRP substrate (Merck-Millipore, Darmstadt, Germany). Details of antibodies and their dilutions used for Western blot analysis are mentioned in Table S7.

Dual-luciferase reporter assay

For the dual-luciferase reporter assay, 50,000 SCC131 or SCC084 cells were seeded in a 24-well plate and were transiently transfected with appropriate plasmid construct(s) as per the experiment requirement. The assay was performed 48 hr post transfection using a Dual-Luciferase® Reporter (DLR™) Assay System kit (Promega, Madison, WI, USA) as per the manufacturer's protocol. The pRL-TK control vector was co-transfected to normalize the transfection efficiency. Each bar is an average of 3 biological replicates and represents relative light units (RLU).

ChIP-qPCR

The ChIP-qPCR was performed using a SimpleChIP® Enzymatic Chromatin IP kit (Magnetic Beads) (Cell Signaling Technology, Danvers, MA, USA) as per manufacturer's instructions. Briefly, 2×10^6 SCC131 cells per 60 mm dish were seeded. Upon reaching ~90% confluency, the cells were cross-linked using 37% formaldehyde per dish (Sigma-Aldrich, St. Louis, MO, USA), following which chromatin was isolated for three IP (immunoprecipitation) reactions using TSC2, IgG, and H3 antibodies. For each ChIP reaction, 5 to 10 µg of digested, cross-linked chromatin was used. After pulldown, all IP reactions were reverse cross-linked, and DNA was purified from each sample which used as template for ChIP-qPCR analysis. The primers were designed to amplify the regions spanning TBSs to check the enrichment of TSC2 on the *MIR514B* promoter (Table S3). The amplification in the IgG-ChIP DNA sample was used as a negative control and was compared to analyse the fold enrichment in TSC2-ChIP DNA. For the positive control, the *RPL30* gene was amplified with H3-ChIP DNA as a template.

Cell proliferation assays

The effect of different construct(s) over proliferation of SCC131 and SCC084 cells was studied by the trypan blue dye exclusion and the BrdU cell proliferation assays. For, trypan blue dye exclusion assay, 2×10^6 cells per well in a 6-well plate were seeded in triplicates and transiently transfected with appropriate plasmid construct(s) using Lipofectamine 2000 transfection reagent. On the day of counting, cell suspension was mixed with 0.4% trypan blue dye (Sigma-Aldrich, St. Louis, MO, USA), loaded onto a Neubauer haemocytometer (HyClone, Logan, UT, USA), and counted using an Olympus CKX4 inverted microscope (Olympus Optical Co., Tokyo, Japan). The total cell number in the original suspension was calculated by the following formula. Number of cells/mL = Average of cells in four quadrants × Dilution factor (10) × 10^4. The live cells were counted every 24 hr for four days, and viable cell number was plotted as a function of time.

For BrdU cell proliferation assay, 2,000 cells per well in quadruplicate in a 96-well plate (3 days, 3 total plates). The cell proliferation was assessed on Day 2, Day 4, and Day 6 using a BrdU cell proliferation assay kit as per the manufacturer's instructions (Merck-Millipore, Darmstadt, Germany).

Caspase-3 activation assay

The apoptosis was measured using a Caspase-3 assay kit (Abcam, Cambridge, UK) as per the manufacturer's instructions. Briefly, 2×10^6 cells per well were seeded in a 6-well plate and transfected using Lipofectamine 2000 with appropriate plasmid construct(s). Post 48 hr, 1 µL of FITC-DEVD label was added to each cell suspension, following which its fluorescence intensity was measured (Ex: 485 nm; Em: 535 nm) using a plate reader (Tecan Group Ltd, Mannedorf, Switzerland).

Anchorage independence assay

The ability of cells to grow in an anchorage independent manner was assessed by the soft agar colony formation assay. After transfecting cells with appropriate constructs, they were harvested and 10,000 cells were plated in 1 mL of 0.5% Noble Agar (BD Difco™, Franklin Lakes, NJ, USA) diluted with culture media in a 35 mm dish. After three weeks, colonies were imaged with a 2.5X objective lens using Leica Inverted Microscope Dmi1 (Leica Microsystems, Wetzlar, Germany) and counted using an image analysis software (Fiji; https://imagej.net/ij/).

AKT inhibitor and rapamycin treatments

For both treatments, 2×10^6 SCC131 or SCC084 cells were seeded in a 6-well plate and treated with 58 nM AKT inhibitor VIII (AKTi) for 24hr or 100 nM rapamycin (MedChemExpress, Princeton, NJ, USA) for 6 hr respectively. DMSO was used as vehicle control in both treatments. After appropriate incubation time, the cells were harvested for total RNA and protein isolation, followed by subsequent experiments.

Statistical analysis

All the experimental data (bar graphs and line diagrams) were plotted using the GraphPad Prism 8 software (https://www.graphpad.com/). The comparison between any two experimental data sets was performed by calculating the statistical significance using Unpaired student's t-test with Welch correction. The comparison among multiple data sets was carried out by performing one-way ANOVA, followed by Tukey's multiple comparison test. The difference among data sets was considered significant when p-values were ≤ 0.05 (*), <0.01 (**), <0.001 (***), <0.0001 (****) or non-significant (ns) when the p-value was >0.05.

Author contributions

SG planned and performed all the experiments, analyzed data, wrote the manuscript and made all figures. NM prepared TSC2 knocked down samples for miRNA microarray. MK assisted in ChIP and cancer hallmark assays. AK supervised the project and edited the manuscript and figures. All authors reviewed and approved the final version of the manuscript.

Conflicts of interest

The authors declare no conflicts of interest.

Data availability statement

All data are available in the manuscript or available upon request.

References

1 Alberts B, Johnson A, Lewis J, Morgan D, Raff M, Roberts K & Walter P (2017) *Molecular Biology of the Cell* (J. Wilson and T. Hunt, eds.) W.W. Norton & Company.

2 Dodd KM & Dunlop EA (2016) Tuberous sclerosis-A model for tumour growth. *Seminars in Cell and Developmental Biology* **52**, 3–11.

3 Fruman DA, Chiu H, Hopkins BD, Bagrodia S, Cantley LC & Abraham RT (2017) The PI3K Pathway in Human Disease. *Cell* **170**, 605–635.

4 Gupta S, Kumar M, Chaudhuri S & Kumar A (2022) The non-canonical nuclear functions of key players of the PI3K-AKT-MTOR pathway. *Journal of Cellular Physiology* **237**, 3181–3204.

5 Rosner M & Hengstschläger M (2007) Cytoplasmic/nuclear localization of tuberin in different cell lines. *Amino Acids* **33**, 575–579.

6 Li Y, Corradetti MN, Inoki K & Guan KL (2004) TSC2: Filling the GAP in the mTOR signaling pathway. *Trends in Biochemical Sciences* **29**, 32–38.

7 Wienecke R, Maize JCJ, Shoarinejad F, Vass WC, Reed J, Bonifacino JS, Resau JH, Gunzburg J de, Yeung RS & DeClue JE (1996) Co-localization of the TSC2 product tuberin with its target Rap1 in the Golgi apparatus. *Oncogene* **13**, 913–923.

8 Clements D, Mayer RJ & Johnson SR (2007) Subcellular distribution of the TSC2 gene product tuberin in human airway smooth muscle cells is driven by multiple localization sequences and is cell-cycle dependent. *American Journal of Physiology - Lung Cellular and Molecular Physiology* **292**, 258–266.

9 Demetriades C, Plescher M & Teleman AA (2016) Lysosomal recruitment of TSC2 is a universal response to cellular stress. *Nature Communications* **7**.

10 Dibble CC, Elis W, Menon S, Qin W, Klekota J, Asara JM, Finan PM, Kwiatkowski DJ, Murphy LO & Manning BD (2012) TBC1D7 is a third subunit of the TSC1-TSC2 complex upstream of mTORC1. *Molecular cell* **47**, 535–546.

11 Henske EP, Jóźwiak S, Kingswood JC, Sampson JR & Thiele EA (2016) Tuberous sclerosis complex. *Nat Rev Dis Primers* **2**, 16035.

12 Laplante M & Sabatini DM (2009) mTOR signaling at a glance. *Journal of Cell Science* **122**, 3589–3594.

13 Neuman NA & Henske EP (2011) Non-canonical functions of the tuberous sclerosis complex-Rheb signalling axis. *EMBO Molecular Medicine* **3**, 189–200.

14 York B, Lou D & Noonan DJ (2006) Tuberin nuclear localization can be regulated by phosphorylation of its carboxyl terminus. *Molecular Cancer Research* **4**, 885–897.

15 Rosner M, Freilinger A & Hengstschläger M (2007) Akt regulates nuclear/cytoplasmic localization of tuberin. *Oncogene* **26**, 521–531.

16 Henry KW, Yuan X, Koszewski NJ, Ondal H, Kwiatkowski DJ & Noonan DJ (1998) Tuberous sclerosis gene 2 product modulates transcription mediated by steroid hormone receptor family members. *Journal of Biological Chemistry* **273**, 20535–20539.

17 Tsuchiya H, Orimoto K, Kobayashi T & Hino O (1996) Presence of potent transcriptional activation domains in the predisposing tuberous sclerosis (Tsc2) gene product of the Eker rat model. *Cancer Research* **56**, 429–433.

18 Pradhan SA, Rather MI, Tiwari A, Bhat VK & Kumar A (2014) Evidence that TSC2 acts as a transcription factor and binds to and represses the promoter of Epiregulin. *Nucleic Acids Research* **42**, 6243–6255.

19 O'Brien J, Hayder H, Zayed Y & Peng C (2018) Overview of MicroRNA Biogenesis, Mechanisms of Actions, and Circulation. *Frontiers in Endocrinology* **9**.

20 Gulyaeva LF & Kushlinskiy NE (2016) Regulatory mechanisms of microRNA expression. *Journal of Translational Medicine* **14**, 143.

21 Wu C, Wang Z, Tian X, Wang J, Zhang Y & Wu B (2021) Long non-coding RNA DDX11-AS1 promotes esophageal carcinoma cell proliferation and migration through regulating the miR-514b-3p/RBX1 axis. *Bioengineered* **12**, 3772–3786.

22 Rosner M, Freilinger A & Hengstschläger M (2007) Akt regulates nuclear/cytoplasmic localization of tuberin. *Oncogene* **26**, 521–531.

23 Ogórek B, Lam HC, Khabibullin D, Liu H-J, Nijmeh J, Triboulet R, Kwiatkowski DJ, Gregory RI & Henske EP (2018) TSC2 regulates microRNA biogenesis via mTORC1 and GSK3β. *Human Molecular Genetics* **27**, 1654–1663.

24 Papadavid E, Braoudaki M, Bourdakou M, Lykoudi A, Nikolaou V, Tounta G, Ekonomidi A, Athanasiadis E, Spyrou G, Antoniou C, Kitsiou-Tzeli S, Rigopoulos D & Kolialexi A (2016) Aberrant microRNA expression in tumor mycosis fungoides. *Tumour Biol* **37**, 14667–14675.

25 Ren L-L, Yan T-T, Shen C-Q, Tang J-Y, Kong X, Wang Y-C, Chen J, Liu Q, He J, Zhong M, Chen H-Y, Hong J & Fang J-Y (2018) The distinct role of strand-specific miR-514b-3p and miR-514b-5p in colorectal cancer metastasis. *Cell Death Dis* **9**, 687.

26 Ma X, Yan W, Xu P, Ma L, Zan Y, Huang L, Wang G, Liu L & Hui W (2022) LncRNA-p21 suppresses cell proliferation and induces apoptosis in gastric cancer by sponging miR-514b-3p and up-regulating ARHGEF9 expression. *Biol Chem* **403**, 945–958.

27 Yang C, Zang Y, Wu S, Zhou Q, Ou Y, Ding Q, Wang H & Xiong Z (2022) Silencing circFTO inhibits malignant phenotype through modulating DUSP4 expression in clear cell renal cell carcinoma. *Cell Death Discov* **8**, 392.

28 Sarkar N & Kumar A (2021) microRNAs: New-Age Panacea in Cancer Therapeutics. *Indian Journal of Surgical Oncology* **12**, 52–56.

29 Gupta S & Kumar A (2025) Tetraspanins: Transcriptional and Post-Transcriptional Regulation and Involvement in Human Health and Diseases. *DNA and Cell Biology Reports* **6**, 82–98.

30 Li PY, Lv J, Qi WW, Zhao SF, Sun LB, Liu N, Sheng J & Qiu WS (2016) Tspan9 inhibits the proliferation, migration and invasion of human gastric cancer SGC7901 cells via the ERK1/2 pathway. *Oncology Reports* **36**, 448–454.

31 Qi Y, Qi W, Liu S, Sun L, Ding A, Yu G, Li H, Wang Y, Qiu W & Lv J (2020) TSPAN9 suppresses the chemosensitivity of gastric cancer to 5-fluorouracil by promoting autophagy. *Cancer Cell Int* **20**, 4.

32 Shao S, Piao L, Wang J, Guo L, Wang J, Wang L, Tong L, Yuan X, Han X, Fang S, Zhu J & Wang Y (2022) Tspan9 Induces EMT and Promotes Osteosarcoma Metastasis via Activating FAK-Ras-ERK1/2 Pathway. *Frontiers in Oncology* **12**.

33 Tan S, Song X, Zhang C, Sun Y, Zhang J, Zhang Z, Zhang R, Zhang T, Zhu X & Tan H (2022) hsa-miR-9-5p-Mediated TSPAN9 Downregulation Is Positively Related to Both Poor Hepatocellular Carcinoma Prognosis and the Tumor Immune Infiltration. *Journal of Immunology Research* **2022**, 1–10.

34 Qi Y, Lv J, Liu S, Sun L, Wang Y, Li H, Qi W & Qiu W (2019) TSPAN9 and EMILIN1 synergistically inhibit the migration and invasion of gastric cancer cells by increasing TSPAN9 expression. *BMC Cancer* **19**, 630.

35 Chen Y & Wang X (2020) miRDB: an online database for prediction of functional microRNA targets. *Nucleic Acids Research* **48**, D127–D131.

36 Agarwal V, Bell GW, Nam J-W & Bartel DP (2015) Predicting effective microRNA target sites in mammalian mRNAs. *eLife* **4**, e05005.

37 Paraskevopoulou MD, Georgakilas G, Kostoulas N, Vlachos IS, Vergoulis T, Reczko M, Filippidis C, Dalamagas T & Hatzigeorgiou AG (2013) DIANA-microT web server

v5.0: service integration into miRNA functional analysis workflows. *Nucleic Acids Research* **41**, W169–W173.

38 Rennie W, Kanoria S, Liu C, Mallick B, Long D, Wolenc A, Carmack CS, Lu J & Ding Y (2016) STarMirDB: A database of microRNA binding sites. *RNA Biology* **13**, 554–560.

39 Sharbati-Tehrani S, Kutz-Lohroff B, Bergbauer R, Scholven J & Einspanier R (2008) miR-Q: a novel quantitative RT-PCR approach for the expression profiling of small RNA molecules such as miRNAs in a complex sample. *BMC Molecular Biology* **9**, 34.

Figure Legends

Fig. 1. TSC2 negatively regulates miR-514b-3p expression in an NLS-dependent manner. (A) Both the transcript and protein levels of TSC2 were downregulated in cells transfected with TSC2 siRNAs as compared to those transfected with Mock siRNAs (n=3). (B) A partial heatmap depicting the top upregulated and downregulated miRNAs identified by miRNA microarray analysis of TSC2 siRNA and Mock siRNA-transfected SCC131 cells. Note, miR-514b-3p is highlighted in a red box. (C) The upregulation of miR-514b-3p in TSC2 siRNAs-transfected SCC131 cells as compared to those transfected with Mock siRNAs (n=3). (D) Nuclear-cytoplasmic fractionation showing the reduction of nuclear TSC2 in pTSC2-NLSdel-transfected cells as compared to those transfected with pTSC2. GAPDH and H3 were used as cytoplasmic and nuclear markers respectively. (E) The downregulation of miR-514b-3p expression in pTSC2-transfected cells as compared to those transfected with pcDNA3.1(+). Note, the upregulation of miR-514b-3p in pTSC2-NLSdel-transfected cells as compared to those transfected with pTSC2 (n=3). (F) TSC2 overexpression in cells transfected with pTSC2 or pTSC2-NLSdel as compared to those transfected with pcDNA3.1(+) (n=3). p value was calculated with Unpaired student's t-test with Welch correction for comparing two data sets and one-way ANOVA, followed by Tukey's multiple comparison test for multiple comparisons. p-values were considered ≤0.05 (*), <0.01 (**), <0.001 (***) <0.0001 (****) and >0.05 (ns).

Fig. 2. TSC2 acts as a transcriptional repressor of miR-514b-3p. (A) A significant promoter activity was observed in SCC131 cells transfected with pPROM-MIR514B as compared to those transfected with the pGL3-Basic vector. pGL3-Basic served as a negative control and pGL3-Control served as a positive control (n=3). (B) The SCC131 cells with the *MIR514B* promoter construct (pPROM-MIR514B) showed a significantly reduced luciferase activity with an increasing dosage of pTSC2 compared to those co-transfected with pPROM-MIR514B

and the pcDNA3.1(+). In addition, the cells with pPROM-MIR514B and pTSC2-NLSdel showed a significantly increased luciferase activity as compared to those co-transfected with pPROM-MIR514B and pTSC2 (n=3). (C) TSC2 shows binding to the five out of seven TBSs (i.e., TBS2, TBS3, TBS4, TBS5, and TBS6) in the *MIR514B* promoter. There was no binding of TSC2 to TBS1, and no amplification was achieved for TBS7. The binding of TSC2 to the *EREG* promoter served as a positive control. All ChIP experiments were plotted as TSC2 fold enrichment in comparison to the IgG control (n=2). p value was calculated with Unpaired student's t-test with Welch correction for comparing two data sets and one-way ANOVA, followed by Tukey's multiple comparison test for multiple comparisons. p-values were considered ≤0.05 (*), <0.01 (**), <0.001 (***) <0.0001 (****) and >0.05 (ns). *Abbreviations*: RLU, Relative light units; TBS, TSC2 binding site; and ChIP, Chromatin immunoprecipitation.

Fig. 3. *TSPAN9* is a direct target of miR-514b-3p. (A) The downregulation of TSPAN9 at both the transcript and protein levels in SCC131 cells transfected with pMIR514B as compared to those transfected with pcDNA3-EGFP (upper and middle panels). Note, upregulation of miR-514b-3p in cells transfected with pMIR514B as compared to those transfected with pcDNA3-EGFP (lower panel). β-actin was used as a loading control (n=3). (B) TSPAN9 showed a concomitant reduction at both transcript and protein levels with an increase in miR-514b-3p expression in a dose-dependent manner (upper and middle panels). Note, concomitant upregulation of miR-514b-3p in cells transfected with pMIR514B as compared to those transfected with pcDNA3-EGFP (lower panel). β-actin was used as loading control (n=3). (C) The dual-luciferase reporter assay showing a direct interaction between the TS in the 3'UTR of *TSPAN9* and the SR of miR-514b-3p in SCC131 cells. Note, a significant decrease in the luciferase activity in cells co-transfected with p3'UTR-TSPAN9 and pMIR514B compared to those transfected with p3'UTR-TSPAN9 and pcDNA3-EGFP. As expected, the cells co-transfected with p3'UTR-RBX and pMIR514B showed significantly reduced luciferase activity compared to those co-transfected with p3'UTR-RBX and pcDNA3-EGFP (n=3). (D) The Western blot analysis showing the levels of TSPAN9 in SCC131 cells transfected with pcDNA3.1(+) only or co-transfected with pMIR514B and pcDNA3.1(+), pMIR514B and pTSPAN9, pMIR514B and pTSPAN9-3'UTR, or pMIR514B and pTSPAN9-3'UTR-M. β-actin was used as loading control. p value was calculated with Unpaired student's t-test with Welch correction for comparing two data sets and one-way ANOVA, followed by Tukey's multiple comparison test for multiple comparisons. p-values were considered ≤0.05 (*), <0.01 (**), <0.001 (***) <0.0001 (****) and >0.05 (ns). *Abbreviations*: RLU, Relative light units

Fig. 4. TSC2 positively regulates the *TSPAN9* expression in an NLS-dependent manner. A) *TSPAN9* showed downregulation in TSC2 siRNAs-transfected SCC131 cells compared to the Mock siRNAs-transfected cells at both transcript and protein levels. Note, TSC2 knockdown was confirmed at protein level (lower panel) (n=3). B) *TSPAN9* showed upregulation in pTSC2-transfected SCC131 cells compared to pcDNA3.1(+)-transfected cells at both transcript and protein levels. Note, *TSPAN9* expression was comparable in pTSC2-NLSdel-transfected cells and the pcDNA3.1(+)-transfected cells. TSC2 overexpression was confirmed at protein level (lower panel) (n=3). p value was calculated with Unpaired student's t-test with Welch correction for comparing two data sets and one-way ANOVA, followed by Tukey's multiple comparison test for multiple comparisons. p-values were considered ≤0.05 (*), <0.01 (**), <0.001 (***) <0.0001 (****) and >0.05 (ns).

Fig. 5. Effects of TSC2, TSPAN9 and miR-514b-3p on proliferation of SCC131 cells. (A-C) The trypan blue dye exclusion assay showing the rate of proliferation of cells transfected with pTSC2, pTSPAN9 or pMIR514B (n=4). (D-F) The BrdU cell proliferation assay showing the rate of proliferation of cells transfected with pTSC2, pTSPAN9 or pMIR514B (n=3). p value was calculated with Unpaired student's t-test with Welch correction. p-values were considered ≤0.05 (*), <0.01 (**), <0.001 (***) <0.0001 (****) and >0.05 (ns).

Fig. 6. miR-514b-3p regulates proliferation, apoptosis, and anchorage-independent growth of SCC131 cells, in part, by targeting the 3'UTR of *TSPAN9*. (A) Effects of miR-514b-3p and different *TSPAN9* constructs on proliferation of SCC131 cells by the Trypan blue dye exclusion assay (n=3) and (B) by the BrdU cell proliferation assay (n=3). (C) Effects of miR-514b-3p and different *TSPAN9* constructs on apoptosis by the Caspase-3 activation assay in SCC131 cells (n=4). (D) Effects of miR-514b-3p and different *TSPAN9* constructs on anchorage-independent growth of SCC131 cells (left panel) and its microscopic images of the soft agar colony formation assay (right panel) (n=3). Scale bar: 500µm. p value was calculated by one-way ANOVA, followed by Tukey's multiple comparison test. p-values were considered ≤0.05 (*), <0.01 (**), <0.001 (***) <0.0001 (****) and >0.05 (ns).

Fig. 7. The miR-514b-3p/TSPAN9 axis regulates the PI3K-AKT-MTOR pathway in OSCC cells. (A) The miR-514b-3p overexpression showed increased levels of pS6K1, PI3K (p55), and pAKT in pMIR514B-transfected cells compared to those transfected with pcDNA3-EGFP. (B) The *TSPAN9* overexpression showed decreased levels of pS6K1, PI3K (p55), and

pAKT in pTSPAN9-transfected cells compared to those transfected with pcDNA3.1(+). β-actin was used as loading control.

Fig. 8. AKT regulates miR-514b-3p/TSPAN9 axis via modulating TSC2 nuclear localization in SCC131 and SCC084 cells. Nuclear-cytoplasmic fractionations showing enhanced nuclear translocation of TSC2 following AKTi treatment of OSCC cells. GAPDH and H3 were used as markers for cytoplasmic and nuclear fractions, respectively (upper panels). The levels of pAKT Ser473 and pTSC2 Ser939 decrease in AKTi treated cells as compared to those treated with the vehicle (upper panels). The miR-514b-3p expression decreases and *TSPAN9* expression increases after AKTi treatment as compared to the vehicle-treated cells (upper and lower panels). β-actin was used as loading control. p value was calculated with Unpaired student's t-test with Welch correction. p-values were considered ≤0.05 (*), <0.01 (**), <0.001 (***) <0.0001 (****) and >0.05 (ns). *Abbreviation:* AKTi, AKT inhibitor VIII.

Fig. 9. TSC2-mediated regulation of miR-514b-3p/TSPAN9 is independent of MTORC1 function. pS6K1 levels were sharply reduced in rapamycin-treated cells as compared to vehicle-treated cells (upper panels). Note, the levels of miR-514b-3p and TSPAN9 do not change after rapamycin treatment as compared to the vehicle treatment of OSCC cells (upper and lower panels). β-actin was used as loading control. p value was calculated with Unpaired student's t-test with Welch correction. p-values were considered ≤0.05 (*), <0.01 (**), <0.001 (***) <0.0001 (****) and >0.05 (ns).

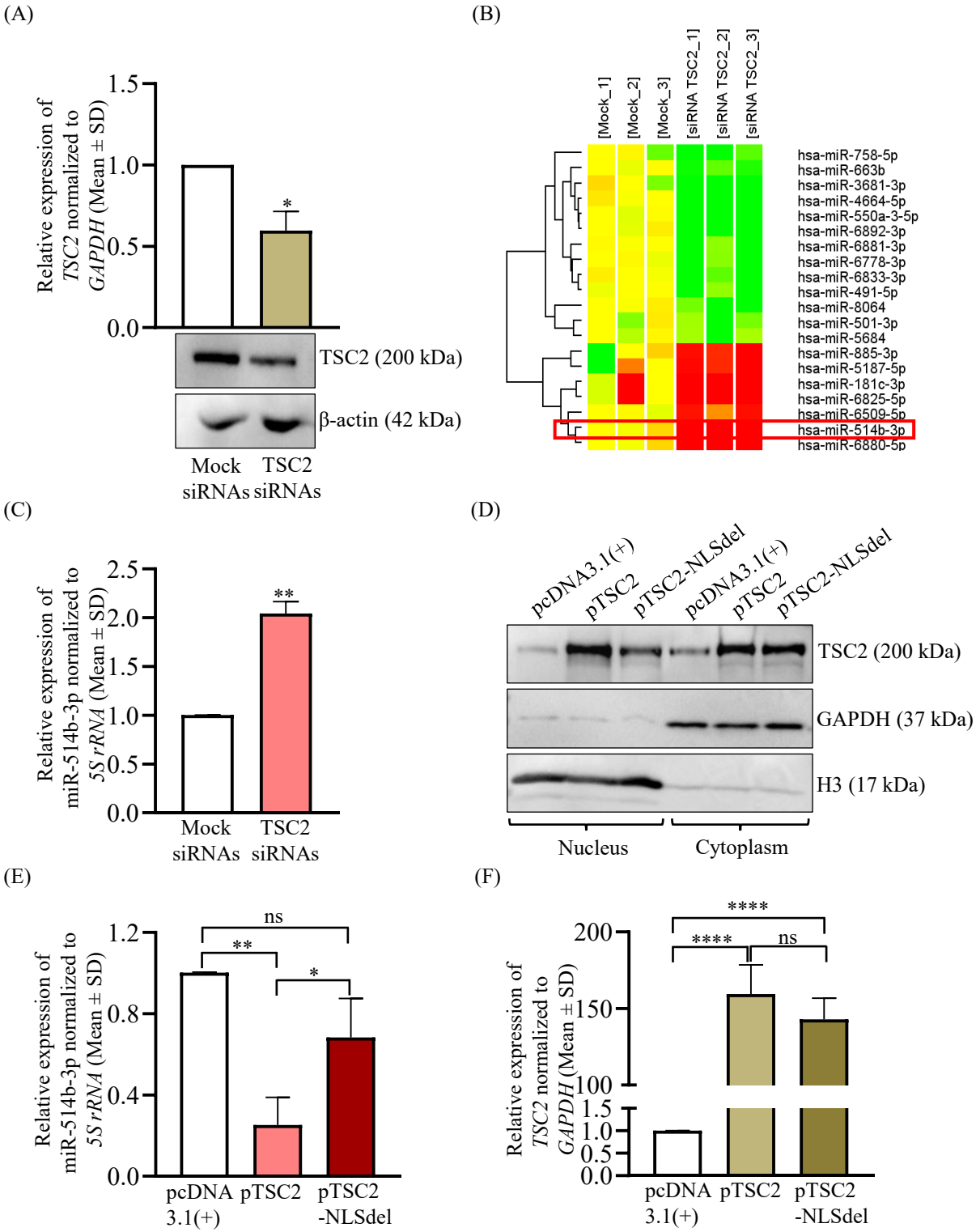
(A)
Relative expression of TSC2 normalized to GAPDH (Mean ± SD)
1.5
1.0
0.5
0.0
*
TSC2 (200 kDa)
β-actin (42 kDa)
Mock siRNAs
TSC2 siRNAs
(B)
[Mock_1]
[Mock_2]
[Mock_3]
[siRNA TSC2_1]
[siRNA TSC2_2]
[siRNA TSC2_3]
hsa-miR-758-5p
hsa-miR-663b
hsa-miR-3681-3p
hsa-miR-4664-5p
hsa-miR-550a-3-5p
hsa-miR-6892-3p
hsa-miR-6881-3p
hsa-miR-6778-3p
hsa-miR-6833-3p
hsa-miR-491-5p
hsa-miR-8064
hsa-miR-501-3p
hsa-miR-5684
hsa-miR-885-3p
hsa-miR-5187-5p
hsa-miR-181c-3p
hsa-miR-6825-5p
hsa-miR-6509-5p
hsa-miR-514b-3p
hsa-miR-6880-5p
(C)
Relative expression of miR-514b-3p normalized to 5S rRNA (Mean ± SD)
2.5
2.0
1.5
1.0
0.5
0.0
**
Mock siRNAs
TSC2 siRNAs
(D)
pcDNA3.1(+)
pTSC2
pTSC2-NLSdel
pcDNA3.1(+)
pTSC2
pTSC2-NLSdel
TSC2 (200 kDa)
GAPDH (37 kDa)
H3 (17 kDa)
Nucleus
Cytoplasm
(E)
Relative expression of miR-514b-3p normalized to 5S rRNA (Mean ± SD)
1.2
0.8
0.4
0.0
ns
**
*
pcDNA 3.1(+)
pTSC2
pTSC2 -NLSdel
(F)
Relative expression of TSC2 normalized to GAPDH (Mean ± SD)
200
150
100
1.5
1.0
0.5
0.0
****
****
ns
pcDNA 3.1(+)
pTSC2
pTSC2 -NLSdel

(A)

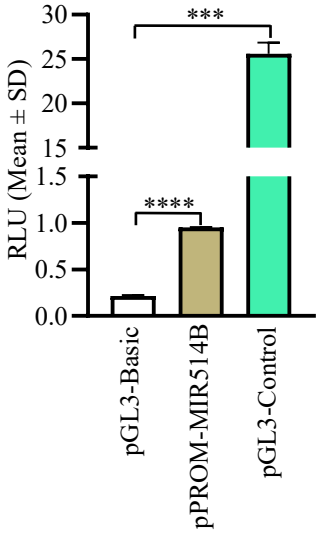
RLU (Mean ± SD)
30
25
20
15
1.5
1.0
0.5
0.0
***
****
pGL3-Basic
pPROM-MIR514B
pGL3-Control

(B)

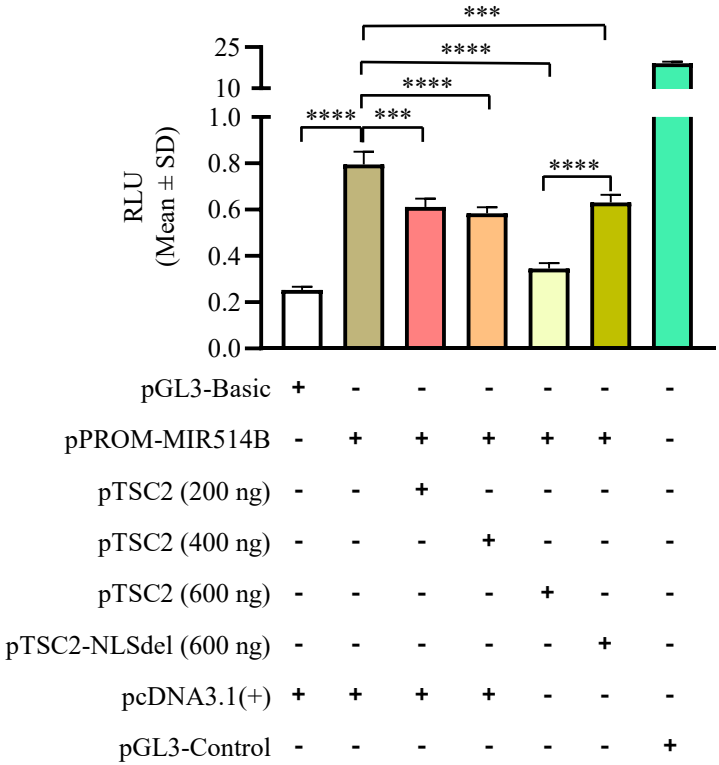
RLU
(Mean ± SD)
25
10
1.0
0.8
0.6
0.4
0.2
0.0
***
****
****
****
***
****
pGL3-Basic + - - - - - -
pPROM-MIR514B - + + + + + -
pTSC2 (200 ng) - - + - - - -
pTSC2 (400 ng) - - - + - - -
pTSC2 (600 ng) - - - - + - -
pTSC2-NLSdel (600 ng) - - - - - + -
pcDNA3.1(+) + + + + - - -
pGL3-Control - - - - - - +

(C)

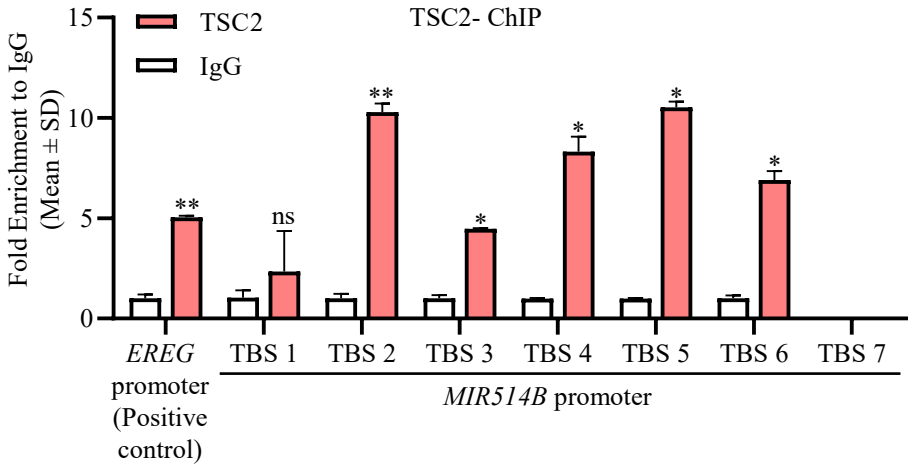
TSC2- ChIP
TSC2
IgG
Fold Enrichment to IgG
(Mean ± SD)
15
10
5
0
**
ns
**
*
*
*
*
EREG
promoter
(Positive
control)
TBS 1
TBS 2
TBS 3
TBS 4
TBS 5
TBS 6
TBS 7
MIR514B promoter

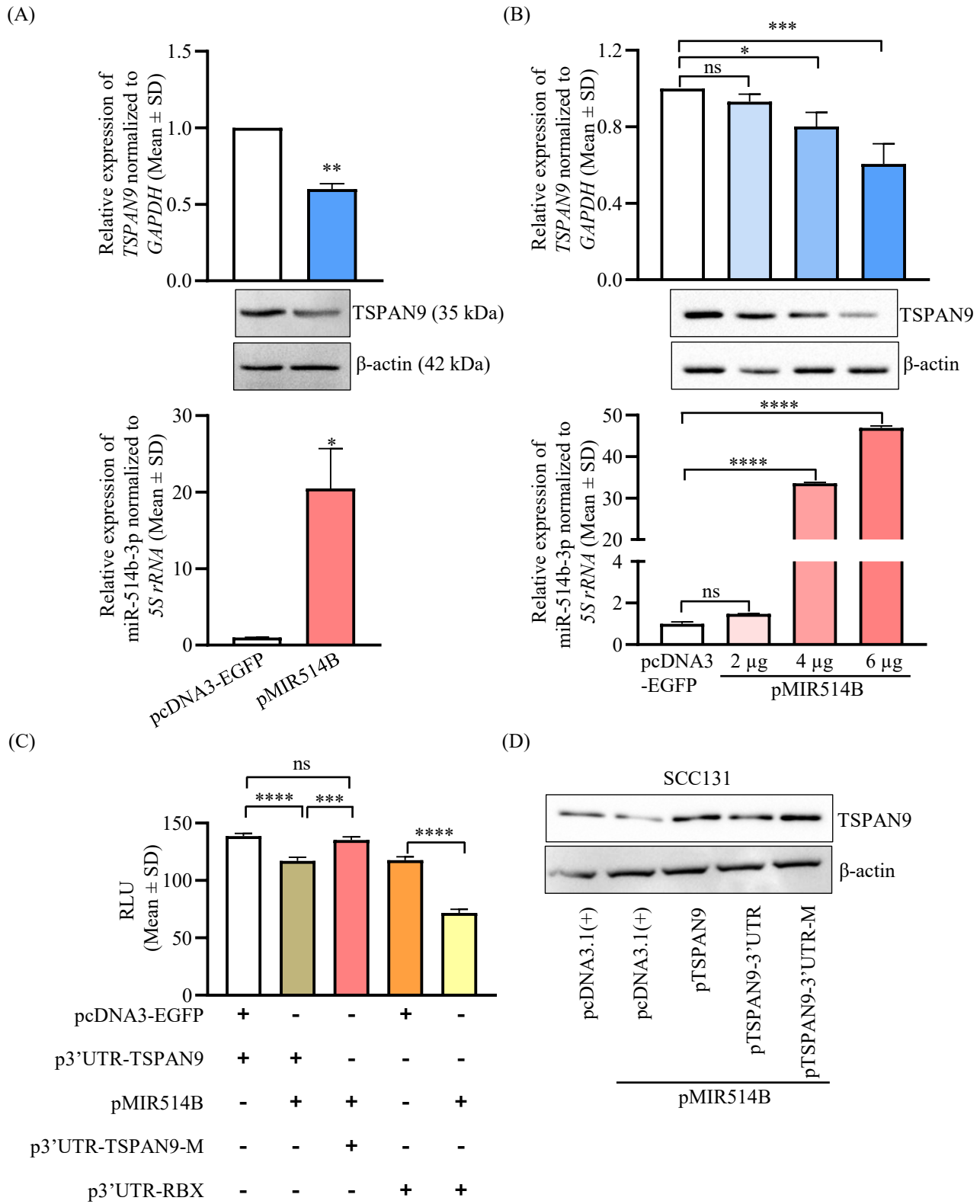
(A)
Relative expression of TSPAN9 normalized to GAPDH (Mean ± SD)
1.5
1.0
0.5
0.0
**
TSPAN9 (35 kDa)
β-actin (42 kDa)
Relative expression of miR-514b-3p normalized to 5S rRNA (Mean ± SD)
30
20
10
0
*
pcDNA3-EGFP
pMIR514B
(B)
Relative expression of TSPAN9 normalized to GAPDH (Mean ± SD)
1.2
0.8
0.4
0.0
***
*
ns
TSPAN9
β-actin
Relative expression of miR-514b-3p normalized to 5S rRNA (Mean ± SD)
50
40
30
20
4
2
0
****
****
ns
pcDNA3 -EGFP
2 μg
4 μg
6 μg
pMIR514B
(C)
RLU (Mean ± SD)
150
100
50
0
ns
****
***
****
pcDNA3-EGFP + - - + -
p3'UTR-TSPAN9 + + - - -
pMIR514B - + + - +
p3'UTR-TSPAN9-M - - + - -
p3'UTR-RBX - - - + +
(D)
SCC131
TSPAN9
β-actin
pcDNA3.1(+)
pcDNA3.1(+)
pTSPAN9
pTSPAN9-3'UTR
pTSPAN9-3'UTR-M
pMIR514B

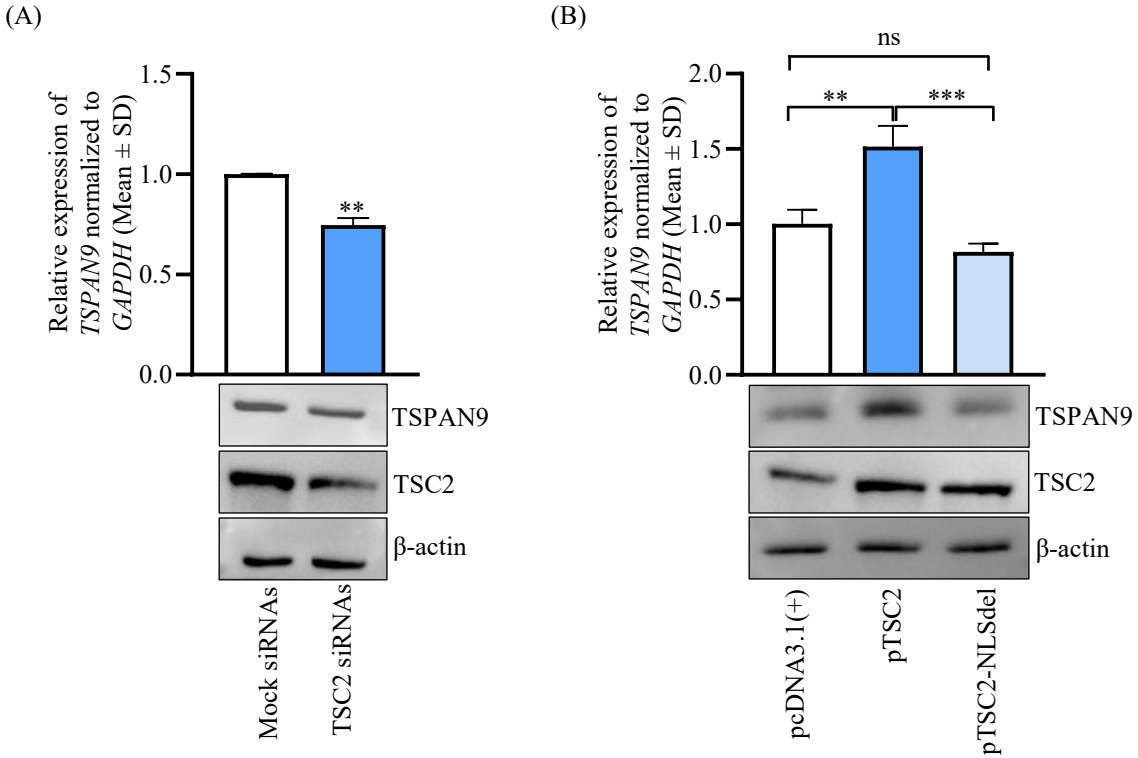
(A)
Relative expression of TSPAN9 normalized to GAPDH (Mean ± SD)
1.5
1.0
0.5
0.0
**
TSPAN9
TSC2
β-actin
Mock siRNAs
TSC2 siRNAs
(B)
ns
**
***
2.0
1.5
1.0
0.5
0.0
TSPAN9
TSC2
β-actin
pcDNA3.1(+)
pTSC2
pTSC2-NLSdel

(A)

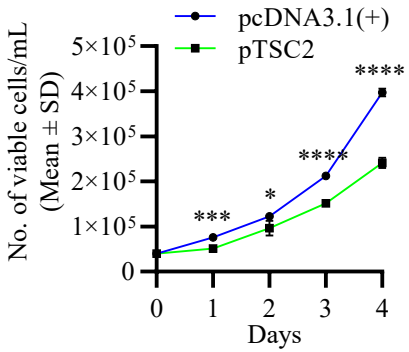
pcDNA3.1(+)
pTSC2
No. of viable cells/mL
(Mean ± SD)
5×10^5
4×10^5
3×10^5
2×10^5
1×10^5
0
***
*
****
****
0
1
2
3
4
Days

(B)

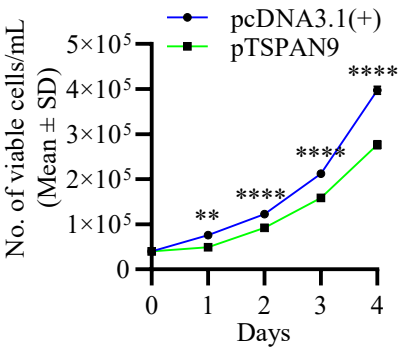
pcDNA3.1(+)
pTSPAN9
No. of viable cells/mL
(Mean ± SD)
5×10^5
4×10^5
3×10^5
2×10^5
1×10^5
0
**
****
****
****
0
1
2
3
4
Days

(C)

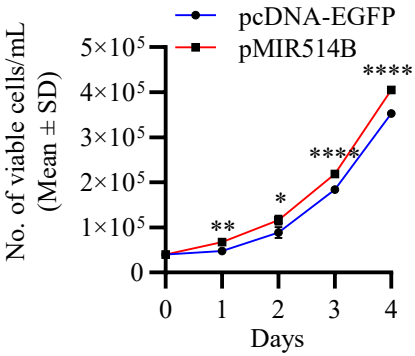
pcDNA-EGFP
pMIR514B
No. of viable cells/mL
(Mean ± SD)
5×10^5
4×10^5
3×10^5
2×10^5
1×10^5
0
**
*
****
****
0
1
2
3
4
Days

(D)

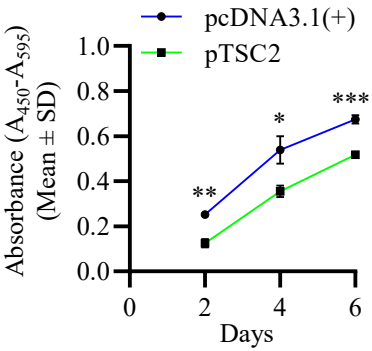
pcDNA3.1(+)
pTSC2
Absorbance (A450-A595)
(Mean ± SD)
1.0
0.8
0.6
0.4
0.2
0.0
**
*
***
0
2
4
6
Days

(E)

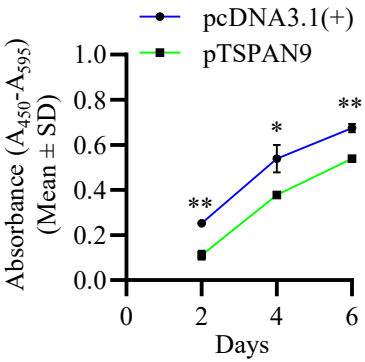
pcDNA3.1(+)
pTSPAN9
Absorbance (A450-A595)
(Mean ± SD)
1.0
0.8
0.6
0.4
0.2
0.0
**
*
**
0
2
4
6
Days

(F)

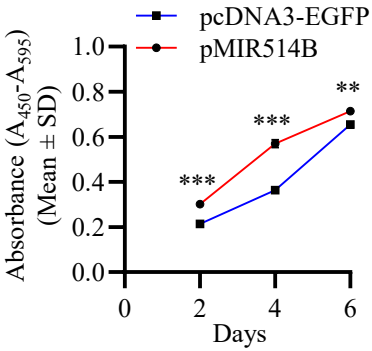
pcDNA3-EGFP
pMIR514B
Absorbance (A450-A595)
(Mean ± SD)
1.0
0.8
0.6
0.4
0.2
0.0
***
***
**
0
2
4
6
Days

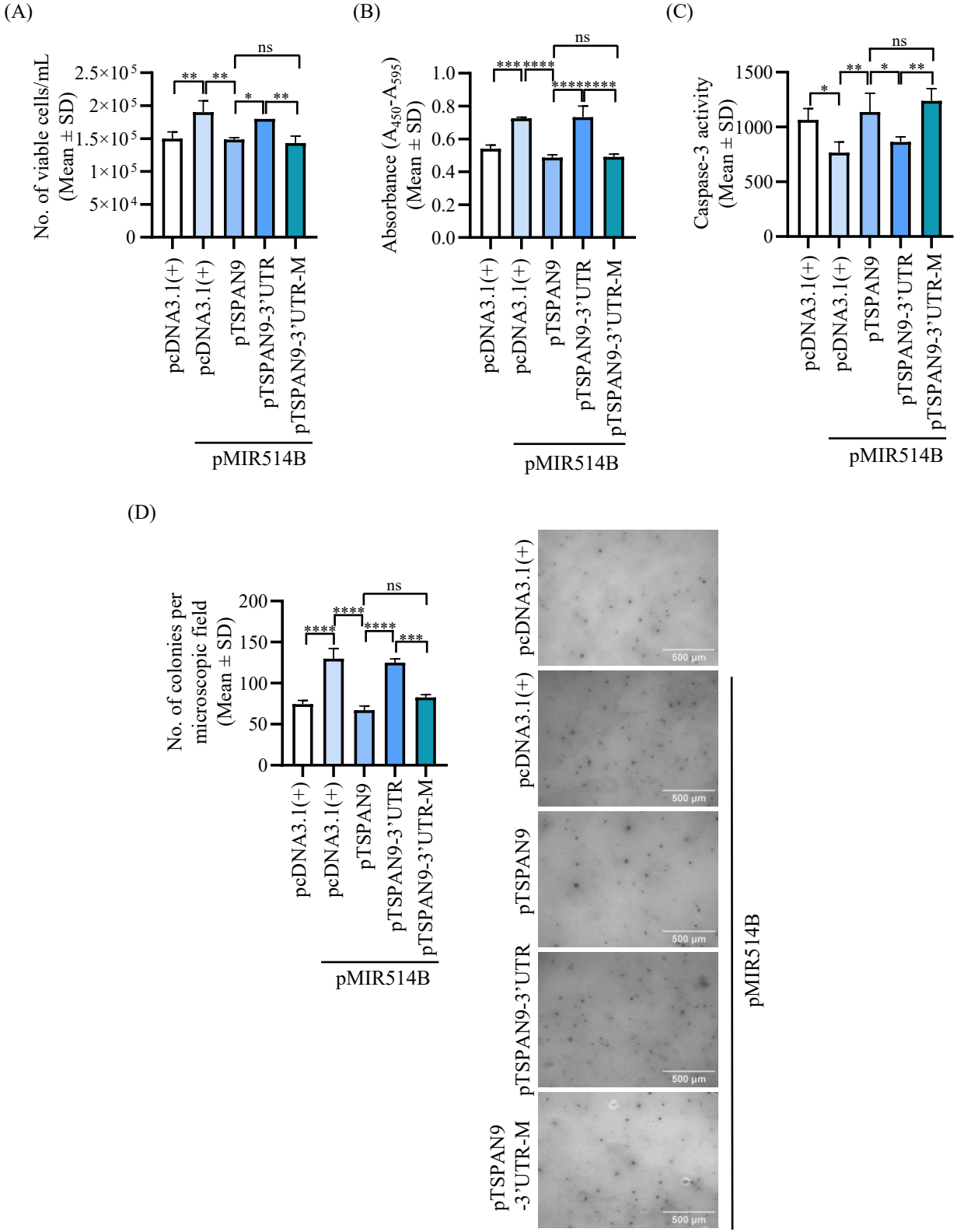
(A)
No. of viable cells/mL (Mean ± SD)
2.5×10^5
2×10^5
1.5×10^5
1×10^5
5×10^4
0
ns
**
**
*
**
pcDNA3.1(+)
pcDNA3.1(+)
pTSPAN9
pTSPAN9-3'UTR
pTSPAN9-3'UTR-M
pMIR514B
(B)
Absorbance (A450-A595) (Mean ± SD)
1.0
0.8
0.6
0.4
0.2
0.0
ns
****
****
pcDNA3.1(+)
pcDNA3.1(+)
pTSPAN9
pTSPAN9-3'UTR
pTSPAN9-3'UTR-M
pMIR514B
(C)
Caspase-3 activity (Mean ± SD)
1500
1000
500
0
ns
*
**
*
**
pcDNA3.1(+)
pcDNA3.1(+)
pTSPAN9
pTSPAN9-3'UTR
pTSPAN9-3'UTR-M
pMIR514B
(D)
No. of colonies per microscopic field (Mean ± SD)
200
150
100
50
0
ns
****
****
****
***
pcDNA3.1(+)
pcDNA3.1(+)
pTSPAN9
pTSPAN9-3'UTR
pTSPAN9-3'UTR-M
pMIR514B
pcDNA3.1(+)
pcDNA3.1(+)
pTSPAN9
pTSPAN9-3'UTR
pTSPAN9 -3'UTR-M
500 μm
pMIR514B

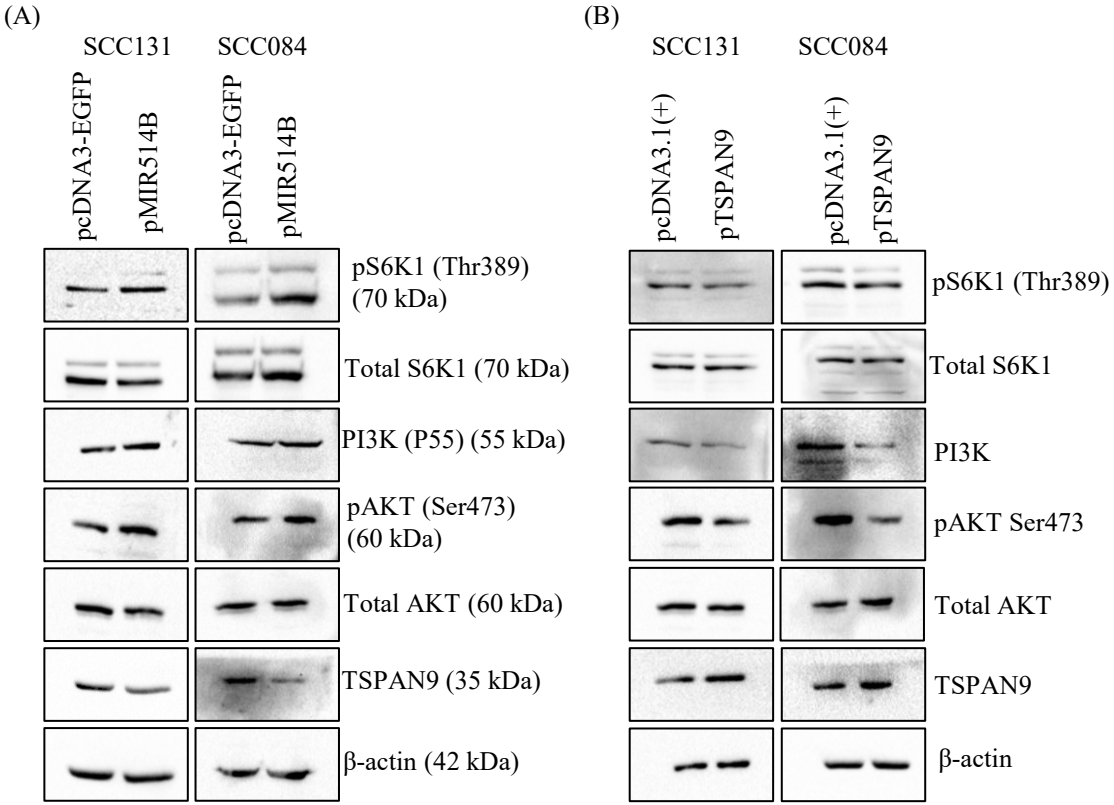
(A)
SCC131
SCC084
pcDNA3-EGFP
pMIR514B
pcDNA3-EGFP
pMIR514B
pS6K1 (Thr389)
(70 kDa)
Total S6K1 (70 kDa)
PI3K (P55) (55 kDa)
pAKT (Ser473)
(60 kDa)
Total AKT (60 kDa)
TSPAN9 (35 kDa)
β-actin (42 kDa)
(B)
SCC131
SCC084
pcDNA3.1(+)
pTSPAN9
pcDNA3.1(+)
pTSPAN9
pS6K1 (Thr389)
Total S6K1
PI3K
pAKT Ser473
Total AKT
TSPAN9
β-actin

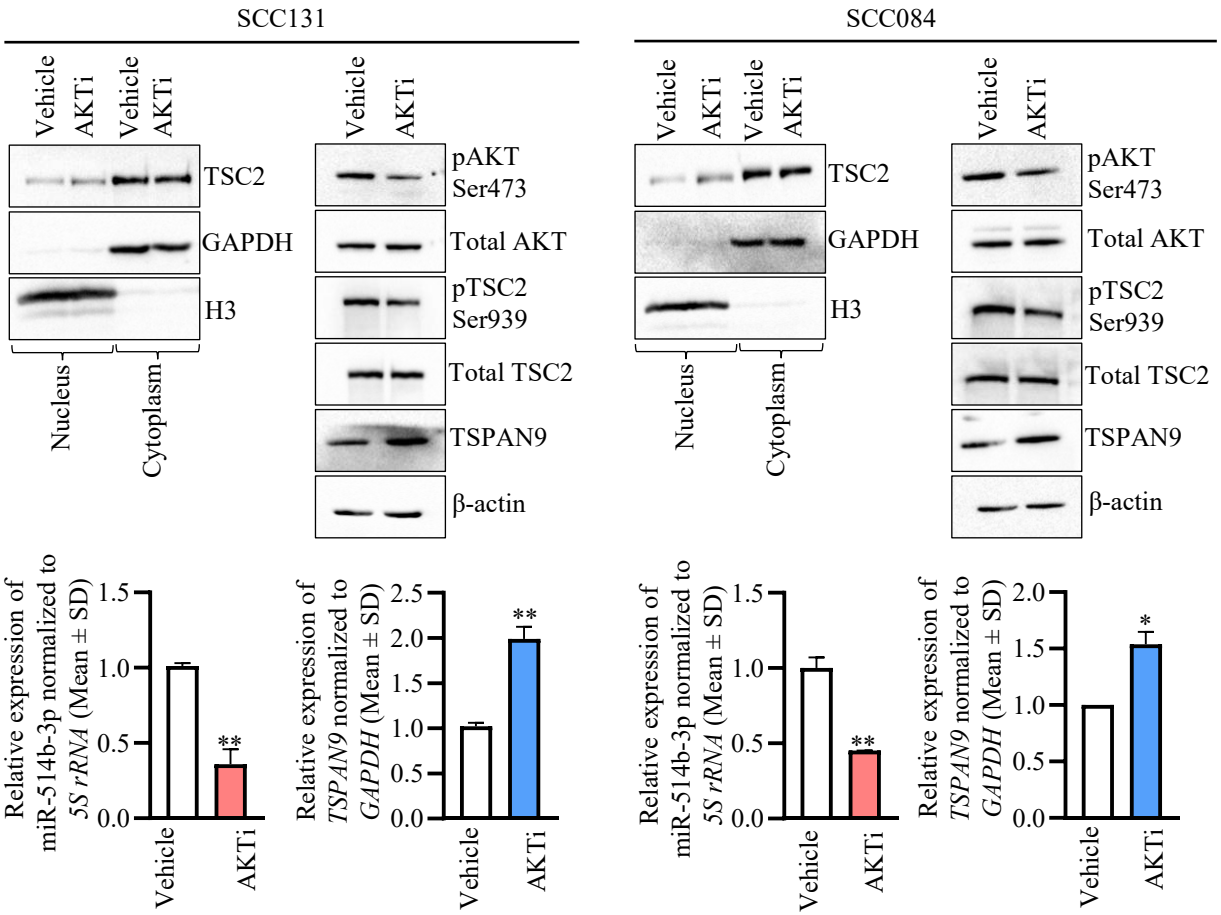
SCC131
SCC084
Vehicle
AKTi
TSC2
GAPDH
H3
Nucleus
Cytoplasm
pAKT Ser473
Total AKT
pTSC2 Ser939
Total TSC2
TSPAN9
β-actin
Relative expression of miR-514b-3p normalized to 5S rRNA (Mean ± SD)
Relative expression of TSPAN9 normalized to GAPDH (Mean ± SD)
**
*

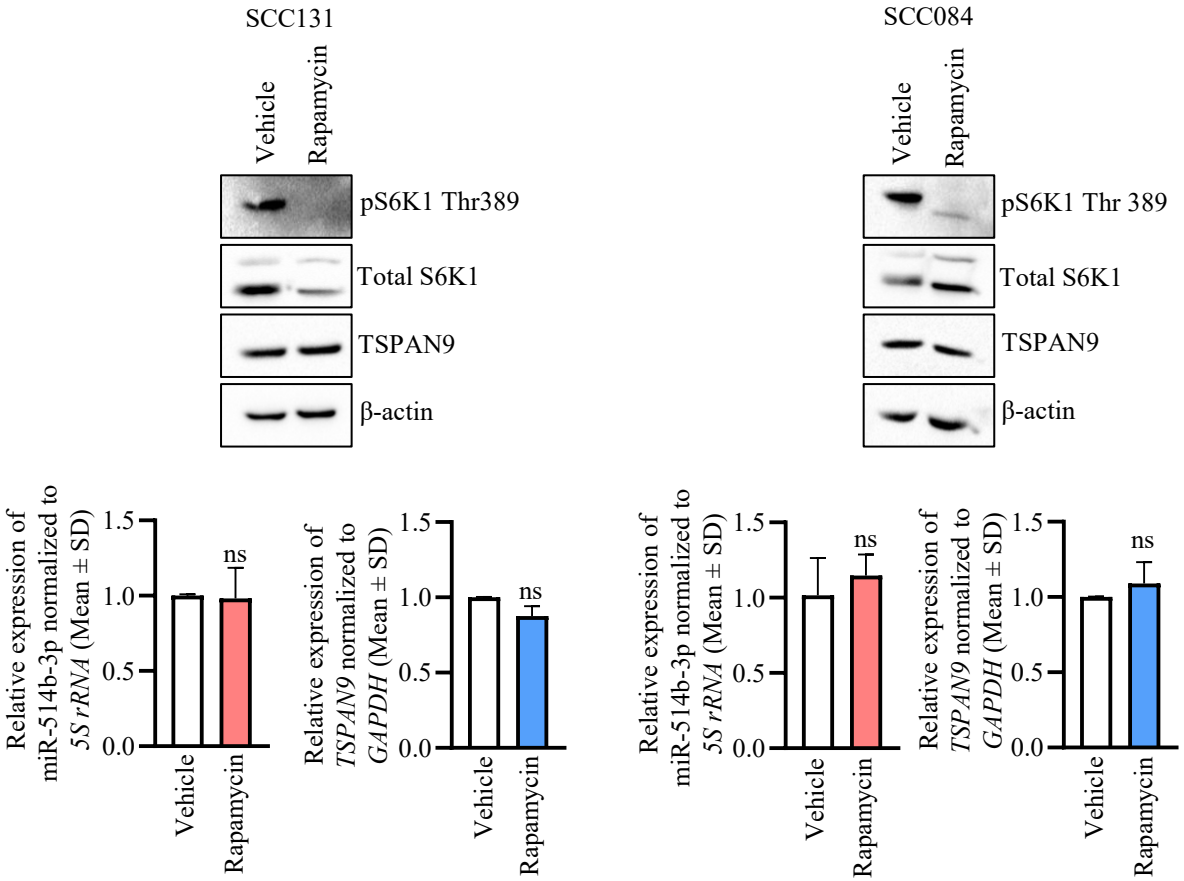
SCC131
Vehicle
Rapamycin
pS6K1 Thr389
Total S6K1
TSPAN9
β-actin
SCC084
Vehicle
Rapamycin
pS6K1 Thr 389
Total S6K1
TSPAN9
β-actin
Relative expression of miR-514b-3p normalized to 5S rRNA (Mean ± SD)
1.5
1.0
0.5
0.0
ns
Vehicle
Rapamycin
Relative expression of TSPAN9 normalized to GAPDH (Mean ± SD)
1.5
1.0
0.5
0.0
ns
Vehicle
Rapamycin
Relative expression of miR-514b-3p normalized to 5S rRNA (Mean ± SD)
1.5
1.0
0.5
0.0
ns
Vehicle
Rapamycin
Relative expression of TSPAN9 normalized to GAPDH (Mean ± SD)
1.5
1.0
0.5
0.0
ns
Vehicle
Rapamycin